Organ-specific Sulfation Patterns of Heparan Sulfate Generated by Extracellular Sulfatases Sulf1 and Sulf2 in Mice

Organ-Specific Sulfation Patterns of Heparan Sulfate Generated by Extracellular Sulfatases Sulf1 and Sulf2 in Mice

Satoshi Nagamine[1, 5, 6], Michiko Tamba[1, 6], Hisako Ishimine[1], Kota Araki[1], Kensuke Shiomi[1], Takuya Okada[1], Tatsuyuki Ohto[1, 2], Satoshi Kunita[3], Satoru Takahashi[3], Ronnie G.P. Wismans[4], Toin H. van Kuppevelt[4], Masayuki Masu[1]*, and Kazuko Keino-Masu[1]*

From the [1]Department of Molecular Neurobiology, [2]Department of Pediatrics, Faculty of Medicine, and [3]Laboratory Animal Resource Center, University of Tsukuba, 1-1-1 Tennodai, Tsukuba, Ibaraki 305-8577, Japan

[4]Department of Matrix Biochemistry, Nijmegen Center for Molecular Life Sciences, Radbout University Nijmegen Medical Center, Nijmegen, The Netherlands

Running title: *Sulfation patterns of heparan sulfate in Sulf knockout mice*

Address correspondence to: Masayuki Masu and Kazuko Keino-Masu, 1-1-1 Tennodai, Tsukuba, Ibaraki 305-8577, Japan; Tel: +81-29-853-3249; Fax: +81-29-853-3498; E-mail: mmasu@md.tsukuba.ac.jp or kazumasu@md.tsukuba.ac.jp

[5]Present address: Department of Neurology, Tokyo Metropolitan Neurological Hospital, 2-6-1 Musashidai, Fuchu, Tokyo 183-0042, Japan

[6]These authors contributed equally to this work.

Background: Extracellular endosulfatases Sulf1 and Sulf2 hydrolyze 6-*O*-sulfate in heparan sulfate.

Results: Disaccharide analysis showed that 2-*O*-, 6-*O*-, and *N*-trisulfated disaccharide units in heparan sulfate were increased to different degrees in different organs in *Sulf1* and *Sulf2* knockout mice.

Conclusion: Sulfs generate organ-specific sulfation patterns of heparan sulfate.

Significance: This may indicate differences in activity between Sulf1 and Sulf2 *in vivo*.

SUMMARY

Heparan sulfate endosulfatases Sulf1 and Sulf2 hydrolyze 6-*O*-sulfate in heparan sulfate, thereby regulating cellular signaling. Previous studies have revealed that Sulfs act predominantly on UA2S-GlcNS6S disaccharides and weakly on UA-GlcNS6S disaccharides. However, the specificity of Sulfs and their role in sulfation patterning of heparan sulfate *in vivo* remained unknown. Here, we performed disaccharide analysis of heparan sulfate in *Sulf1* and *Sulf2* knockout mice. Significant increases in ΔUA2S-GlcNS6S were observed in the brain, small intestine, lung, spleen, testis, and skeletal muscle of adult *Sulf1^{-/-}* mice and in the brain, liver, kidney, spleen, and testis of adult *Sulf2^{-/-}* mice. In addition, increases in ΔUA-GlcNS6S were seen in the *Sulf1^{-/-}* lung and small intestine. In contrast, the disaccharide compositions of chondroitin sulfate were not primarily altered, indicating specificity of Sulfs for heparan sulfate. For *Sulf1*, but not for *Sulf2*, mRNA expression levels in 8 organs of wild-type mice were highly correlated with increases in ΔUA2S-GlcNS6S in the corresponding organs of knockout mice. Moreover, overall changes in heparan sulfate compositions were greater in *Sulf1^{-/-}* mice than in *Sulf2^{-/-}* mice despite lower levels of *Sulf1* mRNA expression, suggesting predominant roles of *Sulf1* in heparan sulfate desulfation and distinct regulation of Sulf activities *in vivo*. *Sulf1* and *Sulf2* mRNAs were differentially expressed in restricted types of cells in organs, and consequently, the sulfation patterns of heparan sulfate were locally and distinctly altered in *Sulf1* and *Sulf2* knockout mice. These findings indicate that Sulf1 and Sulf2 differentially contribute to the generation of organ-specific sulfation patterns of heparan sulfate.

Heparan sulfate (HS) is a long linear carbohydrate chain covalently attached to the core proteins of proteoglycans (1-7). It consists of repeating disaccharide units each composed of an uronic acid (UA: glucuronic acid [GlcA] or iduronic acid [IdoA]) and a glucosamine (*N*-acetylglucosamine [GlcNAc], *N*-sulfated glucosamine [GlcNS], or unsubstituted glucosamine). Each disaccharide has potential sulfation at the 2-*O*-position of UA and the 3-*O*-, 6-*O*-, or *N*-positions of glucosamine (1-7). Because the potential sites are not necessarily all sulfated, HS chains show enormous structural heterogeneity. Typically, HS contains low sulfated regions rich in GlcNAc (NA domain), highly sulfated regions containing contiguous GlcNS (NS domain), and transition zones that contain alternating GlcNAc and GlcNS units (NA/NS domain). After the synthesis of a GlcA-GlcNAc disaccharide polymer, *N*-deacetylase/*N*-sulfotransferases and HS 2-*O*-, 3-*O*-, and 6-*O*-sulfotransferases add sulfate groups to specific sites in the sugar backbone to form complex sulfation patterns (1-7). HS binds to growth factors, enzymes, receptors, and extracellular matrix molecules, thereby regulating many biological processes (1-7). Previous biochemical and genetic studies have shown that specific sulfation patterns of HS are important for the binding to and signaling of these bioactive molecules. Furthermore, distinct sulfation patterns in different tissues at different developmental stages and in different pathological conditions have potential roles in the regulation of cellular signaling (1-7).

Extracellular sulfatases, sulfatase 1 (Sulf1) and sulfatase 2 (Sulf2), catalyze hydrolysis of the sulfate ester bond at the C6 position of glucosamine residues in heparin and HS (8-13). By removing 6-*O*-sulfates in HS, Sulf1 and Sulf2 activate Wnt, Shh, BMP, and GDNF and attenuate the signaling of FGF, VEGF, HGF, and HB-EGF (8, 11, 14-21). Therefore, Sulf1 and Sulf2 are thought to be key regulators of cell proliferation, differentiation, and migration and are also implicated in cancer progression and metastasis (22-23). Biochemical studies have demonstrated that Sulf1 and Sulf2 are most active in the UA2S-GlcNS6S trisulfated disaccharide unit, which is present in the NS domain (9, 11, 13, 16, 24-25). In addition, weaker 6-*O*-desulfation

activity is also detectable in the UA-GlcNS6S disulfated disaccharide unit (11, 24-25). Subsequent disaccharide analysis of embryonic fibroblasts from *Sulf1* and *Sulf2* knockout mice revealed changes suggestive of the specificity of Sulfs towards UA2S-GlcNS6S and UA-GlcNS6S disaccharide units (26). However, how many changes, if any, occur in the disaccharide compositions of HS *in vivo* and whether such changes occur to differing degrees in different organs remain unknown.

The physiological roles of Sulfs *in vivo* have been tested by targeted disruption of *Sulf* genes. Neither *Sulf1*- nor *Sulf2*-deficient mice showed obvious abnormalities despite abundant expression of *Sulf1* and *Sulf2* mRNA in embryonic and adult tissues and the crucial roles HS plays in development and in organ physiology (27-29). In contrast, double knockout mice showed neonatal lethality associated with subtle skeletal abnormalities and kidney hypoplasia (27-29). Defects in esophageal innervation, muscle regeneration, and spermatogenesis were also reported in *Sulf1/2* double knockout mice (27, 30-31). Recently, by using *Sulf1/2* double knockout mice that survived to adulthood (probably owing to differences in genetic background), it was reported that aged double knockout mice developed proteinuria and showed abnormal renal morphology (32).

In this study, we performed systematic disaccharide analysis of HS and chondroitin sulfate (CS) from 8 organs of adult *Sulf1* and *Sulf2* knockout mice. We also determined the expression of *Sulf1* and *Sulf2* mRNA by using RT-PCR and *in sit*u hybridization. These analyses revealed changes in HS disaccharide composition in each organ and their relationship with *Sulf* mRNA expression levels in wild-type mice. Our data provide evidence that Sulf1 and Sulf2 contribute differentially to the generation of organ-specific sulfation patterns of HS *in vivo*.

EXPERIMENTAL PROCEDURES
Materials—Unsaturated HS/HEP-disaccharide mixture (H Mix), Unsaturated Chondro-Disaccharide Kit (C-Kit), heparin lyase II (heparitinase II; *Flavobacterium heparinum*), heparin lyase III (heparitinase I; *Flavobacterium heparinum*), chondroitinase ABC (*Proteus vulgaris*), chondroitinase ACII (*Arthrobacter*

2

aurescens), hyaluronidase (*Streptomyces hyalurolyticus*), CS-A (sturgeon notochord), CS-A (whale cartilage), CS-B (pig skin), CS-C (shark cartilage), CS-D (shark cartilage), CS-E (squid cartilage), and hyaluronic acid (pig skin) were purchased from Seikagaku Biobusiness (Tokyo, Japan). Two standard unsaturated HS disaccharides (ΔUA2S-GlcNAc and ΔUA2S-GlcNAc6S), which are not included in the H Mix, were purchased from Dextra Laboratories (Reading, UK). Heparin lyase I (heparinase I; *Flavobacterium heparinum*), protease type XVI (*Streptomyces griseus*), and Benzonase were purchased from Sigma-Aldrich (St. Louis, MO, USA). Tetra-*n*-butylammonium hydrogen sulfate and 2-cyanoacetamide were purchased from Wako Pure Chemical Industries (Osaka, Japan).

Generation of Sulf-deficient mice—Gene targeting vectors were constructed by inserting the mouse genomic DNA fragments flanking exon 5 of *Sulf1* or *Sulf2* into a TC3 vector (a gift from R. Kageyama), which contained a cassette of stop-IRES-lacZ-polyA, a neomycin-resistant gene, and the diphtheria toxin A fragment gene (Figure S1). The linearized targeting vectors were electroporated into 129/Ola-derived E14 ES cells, and neomycin-resistant colonies selected. Recombinants were identified by PCR, and the correct homologous recombination was then confirmed by Southern blotting. The ES cells obtained were injected into C57BL/6N (CLEA Japan, Tokyo, Japan) blastocysts, and chimeric mice mated with wild-type C57BL/6N mice. Offspring of mice backcrossed to C57BL/6N for 5 successive generations (N5 generation) were used. Genotyping was done by PCR using primer sets of 5'-TGC TGT CCA TCA CGC TCA TCC ATG-3' and 5'-ACC ATC AGG CGA GGG ACTT TTG TC-3' for *Sulf1* and 5'-CGT TGC TAA GGC ACA CAA AG-3' and 5'-GAG CTG ATG TGT GTT TGC TG-3' for *Sulf2*, in combination with a neo primer (5'-CCC TAC CCG GTA GAA TTC GAT ATC-3'). All the experiments using animals were approved by the Animal Care and Use Committee of the University of Tsukuba and performed under its guidelines.

Extraction of glycosaminoglycans—After induction of deep anesthesia by intraperitoneal injection of pentobarbital, 8- to 10-week-old male mice were transcardially perfused with phosphate buffered saline (PBS) to remove blood cells. The brain, lung, liver, spleen, small intestine, kidney, testis, and muscle were isolated and weighed. The organs were then subjected to 3 repeats of homogenization in cooled acetone and centrifugation (2,000 x g for 30 min at 4°C). The precipitates were dried and treated with 10 times the volume of the protease solution (0.8 mg/ml protease type XVI from *Streptomyces griseus* in 50 mM Tris-HCl, pH 8.0, 1 mM CaCl$_2$, 1% TritonX-100, 0.1% BSA) at 55°C overnight. After heat inactivation of the protease at 95°C for 5 min, the solutions were treated with 125 U Benzonase in the presence of 2 mM MgCl$_2$ at 37°C for 2 h. After heat inactivation (95°C for 2 min) and centrifugation (20,000 x g for >30 min at 4°C), the supernatants were filtered with Ultrafree-MC (0.22 μm; Millipore, Billerica, MA, USA) and purified with an anion-exchange column (Vivapure D Mini M; Sartorius, Göttingen, Germany). The eluates were desalted and concentrated using Ultrafree-MC Biomax-5 spin columns. The retentates were vacuum-dried and suspended in 10 μl H$_2$O.

Heparin and chondroitin lyase digestion—For HS analysis, 8 μl of the purified glycosaminoglycans was treated with heparinase I (0.5 U), heparitinase I (1 mIU), and heparitinase II (1 mIU) in 15 μl of a digestion buffer (30 mM sodium acetate, pH 7.0, 3 mM calcium acetate, 0.1% BSA) at 37°C overnight. For CS analysis, 2 μl of the purified glycosaminoglycans was treated with chondroitinase ABC (50 mIU) and chondroitinase ACII (50 mIU) in 15 μl of a digestion buffer (300 mM Tris-acetate, pH 8.0, 0.1% BSA) at 37°C overnight. In some experiments, for removal of hyaluronic acid, the glycosaminoglycans were treated with hyaluronidase (500 TRU) in 20 μl of a digestion buffer (30 mM phosphate buffer, pH 6.0, 0.1% BSA) at 37°C overnight. After heat inactivation at 95°C for 2 min, the digested materials were treated with Ultrafree-MC Biomax-5 spin columns (5,000 nominal molecular weight limit; Millipore), vacuum-dried, suspended in 10 μl H$_2$O, and subjected to CS analysis.

Ion-pair reversed-phase chromatography—Unsaturated disaccharides produced by the enzymatic digestions were analyzed using ion-pair reversed-phase chromatography (33). A

gradient was applied at a flow rate of 1.1 ml/min on a Senshu Pak Docosil column (4.6 x 150 mm, particle size 5 μm; Senshu Scientific, Tokyo, Japan) at 55°C using an HPLC system (Alliance 2695 Separations Module; Waters Corporation, Milford, MA, USA). The eluents used were as follows: A, H$_2$O; B, 0.2 M NaCl; C, 10 mM tetra-*n*-butylammonium hydrogen sulfate; and D, 50% acetonitrile. The gradient program was as follows: 0-10 min, 1-4% eluent B; 10-11 min, 4-15% eluent B; 11-20 min, 15-25% eluent B; 20-22 min, 25-53% eluent B; 22-29 min, 53% eluent B; equilibration with 1% B for 20 min. The proportions of eluent C and D were constant at 12% and 17%, respectively. Aqueous 0.5% (w/v) 2-cyanoacetamide solution and 0.25 M sodium hydroxide were added to the effluent at the same flow rate of 0.35 ml/min using Reagent Managers (Waters). The mixtures were passed through a reaction coil kept at 125°C using a dry reaction temperature-controlled bath (Post-Column Reaction Module; Waters) and Temperature Control Module II (Waters). The effluent was fluorometrically monitored using a multi-wavelength fluorescence detector (Waters 2475 Detector: excitation 346 nm, emission 410 nm; Waters). Disaccharide peaks were identified and quantified by comparison with authentic unsaturated disaccharide markers. The chromatograms were analyzed using Empower 2 software (Waters).

Statistical analysis—Statistical significance of the differences in the disaccharide compositions between the control and single knockout mice was analyzed using the Student's *t* test. First, the *F* test was used to determine whether the variances between the 2 groups were equal. When the variances were equal ($P > 0.05$), an unpaired form of the *t* test was used. When the variances were unequal ($P < 0.05$), Welch's *t* test was used. To analyze the differences among 3 or more groups, ANOVA was performed using PRISM software (GraphPad Software, La Jolla, CA, USA).

RT-PCR—Expression of *Sulf1* and *Sulf2* mRNA in adult mouse organs was determined using quantitative RT-PCR. After decapitation, the brain, lung, liver, spleen, intestine, kidney, testis, and muscle were dissected. Total RNAs were extracted using Sepasol I (Nacalai Tesque, Kyoto, Japan) and purified using an RNeasy kit (Qiagen, Hilden, Germany). Total RNAs (5 μg) were subjected to reverse-transcription using oligo(dT)$_{12-18}$ and Superscript II (Invitrogen, Carlsbad, CA, USA). Quantitative PCR was carried out using a LightCycler and LightCycler FastStart DNA Master SYBR Green I reagent (Roche Diagnostics, Basel, Switzerland). The copy number of each cDNA in the RT solution was determined using standard template DNAs of the pre-determined concentrations. Expression levels were normalized by glyceraldehyde 3-phosphate dehydrogenase (*Gapdh*) expression. The primers used in this study were as follows: *Sulf1*-forward, 5'–CCA TGC TCA CTG GGA AGT ACG TG-3'; *Sulf1*-reverse, 5'–CTT CTC CTT GAT GCC GTT GCG A-3'; *Sulf2*-forward, 5'–AGT GGG TCG GCC TAC TTA AGA ACT C-3'; *Sulf2*-reverse, 5'–ATA GAT CGT CTC CAT GGA GTC A-3'; *Gapdh*-forward, 5'–CAA TGT GTC CGT CGT GGA TCT GAC-3'; *Gapdh*-reverse, 5'–CTG TTG AAG TCG CAG GAG ACA ACC-3'.

Endosulfatase assay—Endosulfatase activities were measured essentially as described previously (34). The 293EBNA cells (Invitrogen) were transfected with pCEP4-*Sulf1-Flag* or pCEP4-*Sulf2-MycHis* with pCEP4-*Sumf1* using Lipofectamine 2000 (Invitrogen). After the cells were cultured in Opti-MEM I (Invitrogen) without fetal bovine serum for 3 days, the conditioned medium was concentrated 30-fold using a Microcon YM-30 filter (Millipore). To measure HS endosulfatase activity, the concentrated conditioned medium (5 μl) was incubated with 10 μg heparin in a total volume of 10 μl of 10 mM Tris-HCl, pH 7.5, 200 mM NaCl, and 10 mM MgCl$_2$ at 37°C for 24 h. The mixture was heated at 95°C for 2 min and then incubated with 1 mIU heparinase I, 1 mIU heparitinase I, and 1 mIU heparitinase II in 10 μl of 40 mM HEPES-NaOH, pH 7.0, and 2 mM calcium acetate at 37°C for 24 h. To measure CS endosulfatase activity, CS-A, CS-B, CS-C, CS-D, or CS-E was incubated with the concentrated conditioned medium and subsequently subjected to digestion by chondroitinase ABC and chondroitinase ACII. After the digestion was stopped by heating at 95°C for 2 min and the mixture cleaned using an Ultrafree-MC filter (Millipore), unsaturated disaccharides were

analyzed by ion-pair reversed-phase chromatography as described above.

In situ hybridization—In situ hybridization was performed essentially as described previously (10). After induction of deep anesthesia, male mice were transcardially perfused with 4% paraformaldehyde (PFA) in PBS. Dissected organs were incubated in the same fixative and subsequently in 30% sucrose/PBS at 4°C overnight. After being embedded in OCT compound (Sakura Finetek, Tokyo, Japan), 10-μm-thick sections were cut using a cryostat (CM1850; Leica Microsystems, Wetzlar, Germany). For the lung, snap frozen tissues were used. The sections were hybridized with 1 μg/ml digoxigenin (DIG)-labeled antisense RNA probe for *Sulf1* or *Sulf2* in a hybridization solution (50% formamide, 5x SSC, pH 4.5, 1% SDS, 50 μg/ml heparin, 50 μg/ml yeast RNA) at 65°C for 16 h. The slides were washed with 50% formamide, 5x SSC, and 1% SDS at 65°C for 30 min; with 50% formamide and 2x SSC at 65°C for 30 min 3 times; and with Tris-HCl, pH 7.6 containing 0.8% NaCl, 0.02% KCl and 0.1% Tween-20 (TBST) at room temperature for 5 min 3 times. After blocking with 0.5% blocking reagent (Roche Diagnostics) in TBST at room temperature for 1 h, the slides were incubated with an alkaline phosphatase-conjugated anti-DIG antibody (1:2000; Roche Diagnostics) in 0.5% blocking reagent in TBST at 4°C for 16 h. After being washed with TBST for 20 min 3 times and with 100 mM Tris-HCl, pH 9.5, 100 mM NaCl, 50 mM $MgCl_2$, and 0.1% Tween-20, signals were detected using BM purple (Roche Diagnostics) in the presence of 2 mM levamisole (Sigma-Aldrich) at room temperature. The RNA probes used in this study contain the sequences 2810-3730 nt for *Sulf1* (NM_001198565.1) and 2396-3208 nt for *Sulf2* (NM_028072.4).

*Immunohistochemistry—*Immunohistochemical detection of HS epitopes was performed essentially as described previously (35-36). Briefly, cryostat sections (10 μm) of snap-frozen tissues were incubated with anti-HS antibodies RB4CD12 and AO4B08 (1:5) in PBS containing 0.5% blocking reagent (Roche Diagnostics) at room temperature for 90 min. After being washed, the sections were incubated with anti-Myc (1:200; Cell Signaling Technology, Danvers, MA, USA)

or anti-VSV-G antibodies (1:200; MBL, Nagoya, Japan) for 60 min. Finally, the slides were incubated with Alexa568-conjugated anti-rabbit IgG (Invitrogen) for 60 min and mounted with coverslips using Fluoromount-G (SouthernBiotech, Birmingham, AL, USA). The images were obtained by means of laser confocal microscopy (LSM510; Carl Zeiss, Jena, Germany). To compare the signal intensities among the different samples, the parameters for image acquisition were kept constant.

RESULTS

Disaccharide compositions of HS in adult mouse organs

To examine the disaccharide compositions of HS *in vivo*, we performed disaccharide analysis of HS in mouse organs (33). Crude extracts of glycosaminoglycans were prepared from the brain, lung, liver, small intestine, kidney, spleen, testis, and skeletal muscle of 8- to 10-week-old male mice. The extracts were exhaustively digested with a mixture of heparin lyases and subjected to ion-pair reversed-phase HPLC (33). This enzyme treatment yielded 8 different unsaturated disaccharides (Figure 1A), 1 unsulfated disaccharide (ΔUA-GlcNAc), 3 monosulfated disaccharides (ΔUA-GlcNS, ΔUA2S-GlcNAc, and ΔUA-GlcNAc6S), 3 disulfated disaccharides (ΔUA2S-GlcNS, ΔUA-GlcNS6S, and ΔUA2S-GlcNAc6S), and 1 trisulfated disaccharide (ΔUA2S-GlcNS6S). The unsaturated disaccharides were fluorometrically detected after post-column reaction with 2-cyanoacetamide. The compositions of the 8 unsaturated disaccharides were compared with the unsaturated HS disaccharide standards and thus quantitatively determined. 3-*O*-sulfated disaccharide units were not detected because they were resistant to heparin lyase digestion. This method allowed sensitive and accurate determination of the sulfation patterns of HS *in vivo*.

The compositions of the HS disaccharides from 8 organs of the wild-type mice were different according to the organ (Figure 1B, Table 1). The percentages were relatively high (>10%) for ΔUA2S-GlcNS6S in the liver (16.7%) and kidney (10.7%), for ΔUA-GlcNS6S in the spleen (14.9%) and kidney (10.7%), for ΔUA2S-GlcNS in the lung (17.2%), brain (14.7%), and testis (13.7%),

and for ΔUA-GlcNAc6S in the spleen (12.6%), kidney (12.2%), and liver (10.1%). These sulfation profiles of HS concur well with those previously reported in mouse and bovine organs (37-40).

Disaccharide compositions of HS in Sulf knockout mice

To examine the roles of *Sulf* genes in generating sulfation patterns of HS *in vivo*, we compared the disaccharide compositions of HS in wild-type and *Sulf* knockout mice (Figure 1C, data not shown). The percentages of trisulfated disaccharide ΔUA2S-GlcNS6S were significantly higher in the brain, small intestine, lung, spleen, testis, and skeletal muscle of *Sulf1* knockout mice (Table 1, Figure 2A). Concomitantly, ΔUA2S-GlcNS decreased significantly in the brain, small intestine, lung, testis, and skeletal muscle of *Sulf1* knockout mice (Table 1). In addition, statistically significant increase in ΔUA-GlcNS6S was observed in the lung and small intestine of *Sulf1* knockout mice, and significant increase in ΔUA-GlcNAc6S in the small intestine (Table 1, Figure 2A). Similar changes in the HS profiles were observed in *Sulf2* knockout mice, but the degree of the changes was smaller than in *Sulf1* knockout mice. Significant increase in ΔUA2S-GlcNS6S was observed in the brain, liver, kidney, spleen, and testis, whereas significant decrease in ΔUA2S-GlcNS was observed in the liver, kidney, and spleen (Table1, Figure 2B). No increase in ΔUA-GlcNS6S or ΔUA-GlcNAc6S was observed in *Sulf2* knockout mice (Table2, Figure 2B).

We also examined the disaccharide compositions of CS in *Sulf* knockout mice. Exhaustive digestion of glycosaminoglycans with chondroitinase ABC and chondroitinase ACII yielded 6 CS unsaturated disaccharides (Figure S2A), 1 unsulfated disaccharide (ΔDi-0S [ΔUA-GalNAc]), 2 monosulfated disaccharides (ΔDi-4S [ΔUA-GalNAc4S], ΔDi-6S [ΔUA-GalNAc6S]), 2 disulfated disaccharides (ΔDi-diS$_D$ [ΔUA2S-GalNAc6S], ΔDi-diS$_E$ [ΔUA-GalNAc4S6S]), and 1 trisulfated disaccharide (ΔDi-triS [ΔUA2S-GalNAc4S6S]). The 8 organs showed unique CS disaccharide patterns (Figure S2B). Quantitative comparison of the CS disaccharides between the *Sulf1* or *Sulf2* knockout mice and the wild-type mice revealed significant increase in ΔDi-6S and ΔDi-diS$_E$ in some organs of the *Sulf1* knockout

mice (Tables S1 and S2), but these changes appeared to be due to secondary effects, as discussed below.

Correlation between Sulf mRNA expression and HS sulfation profiles

Our data indicate that the increase in ΔUA2S-GlcNS6S induced by *Sulf* gene disruption is large in organs possessing relatively low percentages of UA2S-GlcNS6S and relatively high percentages of UA2S-GlcNS in wild-type mice. We thus wondered whether Sulfs trim 6-*O*-sulfate in HS to form organ-specific HS disaccharide compositions, with high levels of *Sulf* expression leading to greater changes in the HS disaccharide composition. To test this, we compared *Sulf* mRNA expression in wild-type mice with changes in ΔUA2S-GlcNS6S of HS in *Sulf* knockout mice.

We first determined the *Sulf* mRNA expression in 8 adult organs by quantitative RT-PCR. In each organ, *Sulf1* mRNA in *Sulf1* heterozygotes was about half that in wild-type mice and negligible in *Sulf1* homozygotes, whereas *Sulf2* mRNA in *Sulf2* heterozygotes was about half that in wild-type mice and negligible in *Sulf2* null mice (Figure S3). In addition, *Sulf1* mRNA levels were unchanged in the *Sulf2* homozygotes except in the liver, whereas *Sulf2* mRNA levels were unchanged in the *Sulf1* homozygotes except in the liver (Figure S3). In the liver, disruption of *Sulf1* led to a 2.4 fold increase in *Sulf2* mRNA (the effects of the *Sulf1* gene disruption were compensated), whereas disruption of *Sulf2* led to a 60% decrease in *Sulf1* mRNA (the effects of the *Sulf2* gene disruption were exaggerated). Such reciprocal regulation of *Sulf* expression may be attributable to the relatively small changes in ΔUA2S-GlcNS6S in the *Sulf1*-deficient liver and relatively large changes in ΔUA2S-GlcNS6S in the *Sulf2*-deficient liver.

Next, we compared the levels of *Sulf1* expression (normalized to *Gapdh* expression) in the wild-type mice and the increase in ΔUA2S-GlcNS6S in the *Sulf1* knockout mice in each organ. As shown in Figure 3A, *Sulf1* expression and ΔUA2S-GlcNS6S increase were proportional and highly correlated ($R = 0.88$). These findings indicate that high levels of *Sulf1* mRNA expression lead to greater degrees of 6-*O*-desulfation. In contrast, no clear correlation was

6

observed between *Sulf2* expression and ΔUA2S-GlcNS6S increase in the *Sulf2* knockout mice (Figure 3B). In this experiment, we calculated the copy numbers of *Sulf1* and *Sulf2* mRNA, allowing the comparison of the absolute levels of *Sulf1/2* mRNA expression. As shown in Figure 3, the overall mRNA expression levels of *Sulf2* were higher than those of *Sulf1*. However, the changes in ΔUA2S-GlcNS6S were smaller in the *Sulf2* knockout mice than in the *Sulf1* knockout mice. These results suggest that *Sulf2* is less active in 6-*O*-desulfation of HS despite higher mRNA expression levels and that *Sulf1* predominantly contributes to the generation of the sulfation patterns of HS in many adult organs.

Disaccharide compositions of HS in Sulf double knockout mice
Given that both Sulf1 and Sulf2 have HS endosulfatase activity *in vitro*, they may be functionally redundant *in vivo*. To test this, we analyzed the disaccharide compositions of HS in *Sulf1/2* double knockout mice. Because the double knockout mice die within 1 day of birth, we used neonatal mice. We analyzed the lung, liver, and kidney because these organs from 1 or 2 neonatal mice gave sufficient HS and CS for the disaccharide analysis. Significant increases in ΔUA2S-GlcNS6S were observed in the lung of *Sulf1* single knockout mice and in the lung and liver of *Sulf2* single knockout mice (Figure 4A, Table 3). In the double knockout mice, ΔUA2S-GlcNS6S was significantly and more robustly increased in the lung, kidney, and liver as compared with in the single knockout mice, indicating that *Sulf1* and *Sulf2* are redundant *in vivo* (Figure 4A, Table 3). The percentages of ΔUA-GlcNS6S were increased in the lung of *Sulf1* single knockout and *Sulf1/2* double knockout mice (Figure 4A, Table 3). However, contrary to the prediction made based on the lack of 6-*O*-desulfation activity in *Sulf* knockout mice, the percentages of ΔUA-GlcNS6S and ΔUA-GlcNAc6S were decreased in the liver of the double knockout mice (Figure 4A, Table 3). These changes are not simply explained by the disruption of 6-*O*-endosulfatase activities and thus can be attributed to secondary changes induced by the disruption of *Sulf1/2* genes.

We next examined the sulfation patterns of CS. Disaccharide analysis of CS showed that ΔDi-diS$_E$ increased in the lung of the *Sulf1* single knockout and *Sulf1/2* double knockout mice, whereas ΔDi-6S increased in the lung of the double knockout mice and the kidney of the *Sulf2* single knockout mice (Figure 4B, Table 3). These results may imply that Sulfs can act on 6-*O*-sulfated disaccharide units in CS. We thus examined whether Sulf1 and Sulf2 have 6-*O*-endosulfatase activity towards CS *in vitro*. In agreement with the results obtained in previous studies including ours (9, 11, 13, 34), when heparin or HS was incubated with a conditioned medium of cells transfected with *Sulf1* or *Sulf2* expression constructs, decreases in ΔUA2S-GlcNS6S and increases in ΔUA2S-GlcNS were observed. In contrast, when CS was incubated with Sulf1 or Sulf2, no changes were observed in the compositions of CS disaccharides in any of the CS subtypes examined (CS-A, CS-B, CS-C, CS-D, and CS-E), indicating that Sulf1 and Sulf2 have no endosulfatase activity towards CS *in vitro* (Figure S4; see also refs 9, 13).

Sulf mRNA expression in organs
We wondered whether *Sulf* genes are broadly expressed and affect global sulfation patterns of HS or whether their expression is rather restricted to specific cell populations and affects local sulfation patterns in adult organs. To examine this, we performed *in situ* hybridization of *Sulf* mRNAs in tissue sections. By using antisense RNA probes against *Sulf1* or *Sulf2*, we could detect specific signals, whereas sense probes yielded no signals (data not shown). In the lung, *Sulf1* mRNA was detected in the blood vessels (most likely the pulmonary arteries), whereas *Sulf2* mRNA was seen in the bronchial wall (Figure 5A-B). In the kidney, *Sulf1* mRNA was strongly detected in the glomeruli (Figure 5C and Figure S5A, C), as reported previously (32, 41). Weak *Sulf1* signals were observed in the blood vessels (Figure S5E). In contrast, *Sulf2* mRNA was seen in a portion of the renal tubules, which, based on the morphological characteristics, were most likely the distal renal tubules (Figure 5D). Moreover, marginal to weak signals of *Sulf2* mRNA were also observed in the glomeruli (Figure S5B, D). In the testis, both *Sulf1* and *Sulf2* mRNAs were seen in the Sertoli cells of the seminiferous tubules in a stage-dependent manner (Figure 5E-F), as reported previously (31).

Therefore, *Sulf* expressions are restricted to particular cell types.

Changes in expression patterns of HS epitopes in Sulf knockout mice

To examine possible changes in the sulfation patterns of HS at the cell level, we performed immunohistochemistry of HS by using a set of phage display-derived antibodies (35-36). Biochemical and histological studies have shown that these antibodies recognize different epitopes in HS chains and are therefore useful for examining the heterogeneity of HS *in vivo* (35-36). We selected 2 well-characterized antibodies, AO4B08 and RB4CD12. AO4B08 reacts with heavily *O*-sulfated NS domains composed of at least 3 disaccharide units (36). RB4CD12 recognizes *N*- and *O*-sulfated HS epitopes, which are subjected to degradation by Sulfs (42).

We first examined the localization of the HS epitopes in the kidney because previous studies have revealed *Sulf1/2* double knockout led to renal hypoplasia in neonates and glomerular abnormalities and proteinuria in aged animals (28, 32). In the wild-type mice, RB4CD12 strongly stained the renal tubules and Bowman's capsules and weakly stained the glomeruli (Figure 6A). AO4B08 stained the renal tubules and Bowman's capsules, but not the glomeruli (Figures 6D), as reported previously (36). Next we examined the staining patterns in the kidneys of *Sulf1* and *Sulf2* knockout mice. In the *Sulf1* knockout mice, RB4CD12 staining was slightly increased in the glomeruli, whereas increases in AO4B08 staining in the glomeruli were small, if any at all (Figure 6B, E). In one of the *Sulf1* knockout mice, strong punctate signals of AO4B08 were observed in the glomeruli (Figure S6B). In the *Sulf2* knockout mice, neither of the 2 antibodies showed increases in the glomerular signals (Figure 6C, F). Given the specific and robust expression of *Sulf1* mRNA in the glomeruli, these findings indicate that the localized changes in HS disaccharide composition occurred as a result of *Sulf1* disruption. We could not see obvious increases in anti-HS staining intensity in the renal tubules of *Sulf* knockout mice probably because the staining in the renal tubules in the wild-type mice was so strong that it was hard to detect subtle changes in the staining intensity by immunohistochemistry. To detect possible changes in the renal tubules, we performed titration experiments. When stained by

diluted antibodies (1:50 dilution instead of the 1:5 dilution used in other experiments), no obvious increases were observed in any regions in the *Sulf* knockout kidneys except for increases in the AO4B08 signals in the blood vessels of *Sulf1* knockout mice (Figure S7). In the lung, both RB4CD12 and AO4B08 staining appeared to increase in the blood vessels of the *Sulf1* knockout mice (Figure S8), although precise quantitation of the change in the signal intensity was difficult.

Finally we examined the changes in HS staining in neonatal mice. In the lung, both RB4CD12 and AO4B08 staining appeared to increase in the blood vessels of *Sulf1* knockout mice and more robustly in those of double knockout mice (Figure 7). In the kidney of neonatal wild-type mice, both RB4CD12 and AO4B08 signals were observed in the glomeruli (Figure S9A, E). RB4CD12 staining appeared to be slightly increased in the double knockout mice (Figure S9D).

DISCUSSION

We here performed systematic disaccharide analysis of HS in *Sulf1* and *Sulf2* knockout mice. As predicted from the *in vitro* activities of Sulfs, ΔUA2S-GlcNS6S was increased, and ΔUA2S-GlcNS concomitantly decreased in *Sulf*-deficient organs. However, the degree of change was different from organ to organ and between *Sulf1* and *Sulf2* knockout mice. In general, the increase in ΔUA2S-GlcNS6S was large in organs that showed relatively low percentages of ΔUA2S-GlcNS6S and relatively high percentages of ΔUA2S-GlcNS in wild-type mice. These findings indicate that the HS disaccharide profiles that are characteristic to each organ, especially the low ΔUA2S-GlcNS6S patterns, are attributable to HS 6-*O*-desulfation by Sulfs. Therefore, in addition to HS 6-*O*-sulfotransferases (43), Sulfs contribute to generating organ-specific sulfation patterns of HS.

In addition to the increase in ΔUA2S-GlcNS6S, ΔUA-GlcNS6S was also increased, to a lesser extent but significantly, in the lung and small intestine of adult *Sulf1* knockout mice as well as in the lungs of neonatal *Sulf1* knockout and *Sulf1/Sulf2* double knockout mice. Given that Sulf1/2 can hydrolyze 6-*O*-sulfate in UA-GlcNS6S disaccharide units in HS *in vitro* (11,

24-25), these findings suggest the possibility that Sulfs act on UA-GlcNS6S disaccharide units in some organs. Because the *Sulf1* expression is highest in the lung, high endosulfatase activity may lead to desulfation of UA-GlcNS6S disaccharide units. Or, a specific oligosaccharide sequence that contains UA-GlcNS6S disaccharide units and undergoes desulfation by Sulfs may be abundant in the lung and small intestine.

We also noted changes in HS and CS disaccharide compositions that were not predicted from *in vitro* studies. HS disaccharide ΔUA-GlcNAc6S was increased in the small intestine of *Sulf1* knockout mice, and CS disaccharide ΔDi-diS$_E$ in the lungs of adult and neonatal *Sulf1* knockout mice as well as of *Sulf1/Sulf2* double knockout mice. These increases may simply mean that Sulfs have 6-*O*-endosulfatase activities towards these disaccharide units. However, given that HS 6-*O*-endosulfatase activity towards UA-GlcNAc6S units has never been detected *in vitro* (9, 11, 13, 24-25, 34) and that Sulfs show no endosulfatase activity towards CS (this study; see also refs 9, 13), these changes seem to have occurred as a secondary consequence of alteration of the HS sulfation patterns, although the possibility cannot be formally excluded that Sulfs acquire such activity in collaboration with unknown factor(s) *in vivo*. Interestingly, Sulf1 and Sulf2 have different degrees of impact on 6-*O*-sulfation states of HS *in vivo*, although they have indistinguishable activity *in vitro*. For example, although *Sulf2* mRNA expression was about 3-fold higher than that of *Sulf1* mRNA in the lung, increases in ΔUA2S-GlcNS6S in *Sulf2*-knockout mice were trivial (5.5%) in contrast to large (126%) increases in ΔUA2S-GlcNS6S in *Sulf1*-knockout mice. Although the specific activities of Sulf1 and Sulf2 (6-*O*-desulfation activity per unit protein) have not been determined, if we assume that they have the same specific activity, these data suggest that Sulf1 and Sulf2 function in a different fashion *in vivo*. The following are possible causative factors for the differences. First, Sulf2 may be more labile than Sulf1, and the steady state levels of Sulf2 may be low. The levels of Sulf1 and Sulf2 proteins should be determined and compared with the changes in HS composition in future. Second, the activity of Sulf2 can be inhibited by unknown factor(s) in normal conditions. Third, Sulf1 protein may be

more diffusible and thus able to desulfate more HS. Given that the cleavage of Sulf proteins by furin-type proteinases affects the accumulation of Sulf proteins in lipid-rich domains as well as Wnt activation (44), Sulf1 and Sulf2 may undergo different protein cleavage *in vivo*. Although Sulf1 and Sulf2 show overall sequence similarity, the hydrophilic domains in their middle portions are divergent (22). Because the hydrophilic domains are required for secretion and cell surface localization of Sulf proteins (13, 22), these sequences may give rise to the functional differences between these 2 Sulf proteins. Fourth, Sulf2 may be localized apart from the target HS. Fifth, native HS may contain certain oligosaccharide structures that are more vulnerable to desulfation by Sulf1. Future studies are required to elucidate the molecular mechanisms that lead to the functional differences between Sulf1 and Sulf2 *in vivo*.

We showed that the composition of HS changed at the cell level as a result of *Sulf* gene disruption. In the kidney glomeruli, the RB4CD12 epitope and (to a lesser extent) AO4B08 epitope increased in adult *Sulf1* knockout mice. Because both AO4B08 and RB4CD12 react with trisulfated disaccharide motifs in HS (45) and because *Sulf1* mRNA is expressed specifically in the glomeruli of adult kidneys, these findings indicate that Sulf1 remodels sulfation profiles of HS locally. In the disaccharide analysis, however, increases in ΔUA2S-GlcNS6S were not significant in the *Sulf1* knockout kidney. This is likely because the increases in ΔUA2S-GlcNS6S in the glomeruli were masked when analyzed at the organ level. Conversely, in the *Sulf2* knockout mice, we could not see any obvious changes in anti-HS staining in the renal tubules, whereas increases in ΔUA2S-GlcNS6S were significant in the *Sulf2* knockout kidney. It is likely that strong anti-HS signals in the renal tubules hamper the detection of probable changes in the staining, although it is also possible that the antibodies used in this study did not recognize the increased ΔUA2S-GlcNS6S-containing HS domains. Thus, the combination of biochemical analysis of HS disaccharide profiles and immunohistochemical analysis by anti-HS antibodies would be useful for elucidating where and how HS regulates cell signaling and how *Sulfs* are involved in the processes *in vivo*. In the lung, increases in

9

RB4CD12/AO4B08 staining were robust in the blood vessels of *Sulf1* knockout mice as well as of double knockout mice. Given that RB4CD12 staining in wild-type mice is strong in the blood vessels of the mouse brain (46), Sulf1 may regulate vascular signaling in general. Therefore, future studies are necessary to unravel the possible roles of *Sulf1* in the physiology and pathology of the vascular system.

Although accumulating evidence has suggested that Sulfs regulate multiple signaling pathways *in vitro*, the functional consequences of *Sulf* gene disruption are small. Mice deficient in either *Sulf1* or *Sulf2* are healthy and appear to be normal (27-29) except for some subtle phenotypes. The body weight of *Sulf2* knockout mice is smaller than those of wild-type and *Sulf1* knockout mice (28; S.N., K.K-M., and M.M., unpublished data). *Sulf2* mutant mice generated by gene trapping occasionally showed defects in the lung (47). In contrast, double knockout mice die postnatally, indicating overlapping and essential roles of *Sulf* genes in mouse development. Double knockout mice showed reduced body weight, kidney hypoplasia, and skeletal abnormalities (27-29; S.N., K.K-M., and M.M., unpublished data). In embryonic kidneys, *Sulf1* mRNA is expressed in the developing glomeruli, whereas *Sulf2* mRNA is expressed in the nephron progenitors and tubules (32). Thus Sulfs likely regulate cell differentiation and/or proliferation in kidneys, although more studies are required to elucidate the molecular mechanisms by which Sulfs play roles in kidney development. Recently, by using double knockout mice that survived to adulthood, it was shown that simultaneous disruption of *Sulf1* and *Sulf2* genes led to proteinuria and glomerular defects in aged animals (32). Clearly the phenotype seems to be associated with changes in HS sulfation in the glomeruli in *Sulf1* knockout mice, although we did not examine the HS profiles of adult double knockout mice owing to their neonatal lethality. Utilization of such double knockout mice may facilitate the understanding of the roles of *Sulf* genes and 6-*O*-desulfation *in vivo*.

REFERENCES

1. Lindahl, U., Kusche-Gullberg, M., and Kjellen, L. (1998) *J. Biol. Chem.* **273**, 24979-24982
2. Bernfield, M., Götte, M., Park, P. W., Reizes, O., Fitzgerald, M. L., Lincecum, J., and Zako, M. (1999) *Annu. Rev. Biochem.* **68**, 729-777
3. Gallagher, J. T. (2001) *J. Clin. Invest.* **108**, 357-361
4. Turnbull, J., Powell, A., and Guimond, S. (2001) *Trends Cell Biol.* **11**, 75-82
5. Esko, J. D., and Selleck, S. B. (2002) *Annu. Rev. Biochem.* **71**, 435-471
6. Bülow, H. E., and Hobert, O. (2006) *Annu. Rev. Cell Dev. Biol.* **22**, 375-407
7. Bishop, J. R., Schuksz, M., and Esko, J. D. (2007) *Nature* **446**, 1030-1037
8. Dhoot, G. K., Gustafsson, M. K., Ai, X., Sun, W., Standiford, D. M., and Emerson, C. P., Jr. (2001) *Science* **293**, 1663-1666
9. Morimoto-Tomita, M., Uchimura, K., Werb, Z., Hemmerich, S., and Rosen, S. D. (2002) *J. Biol. Chem.* **277**, 49175-49185
10. Ohto, T., Uchida, H., Yamazaki, H., Keino-Masu, K., Matsui, A., and Masu, M. (2002) *Genes Cells* **7**, 173-185
11. Ai, X., Do, A. T., Lozynska, O., Kusche-Gullberg, M., Lindahl, U., and Emerson, C. P., Jr. (2003) *J. Cell Biol.* **162,** 341-351
12. Nagamine, S., Koike, S., Keino-Masu, K., and Masu, M. (2005) *Brain Res. Dev. Brain Res.* **159**, 135-143
13. Ai, X., Do, A. T., Kusche-Gullberg, M., Lindahl, U., Lu, K., and Emerson, C. P., Jr. (2006) *J. Biol. Chem.* **281**, 4969-4976
14. Lai, J., Chien, J., Staub, J., Avula, R., Greene, E. L., Matthews, T. A., Smith, D. I., Kaufmann, S. H., Roberts, L. R., and Shridhar, V. (2003) *J. Biol. Chem.* **278**, 23107-23117
15. Lai, J. P., Chien, J. R., Moser, D. R., Staub, J. K., Aderca, I., Montoya, D. P., Matthews, T. A., Nagorney, D. M., Cunningham, J. M., Smith, D. I., Greene, E. L., Shridhar, V., and Roberts, L. R.

(2004) *Gastroenterology* **126**, 231-248

16. Viviano, B. L., Paine-Saunders, S., Gasiunas, N., Gallagher, J., and Saunders, S. (2004) *J. Biol. Chem.* **279**, 5604-5611

17. Wang, S., Ai, X., Freeman, S. D., Pownall, M. E., Lu, Q., Kessler, D. S., and Emerson, C. P., Jr. (2004) *Proc. Natl. Acad. Sci. U.S.A.* **101**, 4833-4838

18. Danesin, C., Agius, E., Escalas, N., Ai, X., Emerson, C., Cochard, P., and Soula, C. (2006) *J. Neurosci.* **26**, 5037-5048

19. Uchimura, K., Morimoto-Tomita, M., Bistrup, A., Li, J., Lyon, M., Gallagher, J., Werb, Z., and Rosen, S. D. (2006) *BMC Biochem.* **7**, 2

20. Ai, X., Kitazawa, T., Do, A. T., Kusche-Gullberg, M., Labosky, P. A., and Emerson, C. P., Jr. (2007) *Development* **134**, 3327-3338

21. Freeman, S. D., Moore, W. M., Guiral, E. C., Holme, A. D., Turnbull, J. E., and Pownall, M. E. (2008) *Dev. Biol.* **320**, 436-445

22. Lamanna, W. C., Kalus, I., Padva, M., Baldwin, R. J., Merry, C. L., and Dierks, T. (2007) *J. Biotechnol.* **129**, 290-307

23. Rosen, S. D., and Lemjabbar-Alaoui, H. (2010) *Expert Opin. Ther. Targets* **14**, 935-949

24. Lamanna, W. C., Frese, M. A., Balleininger, M., and Dierks, T. (2008) *J. Biol. Chem.* **283**, 27724-27735

25. Frese, M. A., Milz, F., Dick, M., Lamanna, W. C., and Dierks, T. (2009) *J. Biol. Chem.* **284**, 28033-28044

26. Lamanna, W. C., Baldwin, R. J., Padva, M., Kalus, I., Ten Dam, G., van Kuppevelt, T. H., Gallagher, J. T., von Figura, K., Dierks, T., and Merry, C. L. (2006) *Biochem. J.* **400**, 63-73

27. Ai, X., Kitazawa, T., Do, A. T., Kusche-Gullberg, M., Labosky, P. A., and Emerson, C. P., Jr. (2007) *Development* **134**, 3327-3338

28. Holst, C. R., Bou-Reslan, H., Gore, B. B., Wong, K., Grant, D., Chalasani, S., Carano, R. A., Frantz, G. D., Tessier-Lavigne, M., Bolon, B., French, D. M., and Ashkenazi, A. (2007) *PLoS One* **2**, e575

29. Ratzka, A., Kalus, I., Moser, M., Dierks, T., Mundlos, S., and Vortkamp, A. (2008) *Dev. Dyn.* **237**, 339-353

30. Langsdorf, A., Do, A. T., Kusche-Gullberg, M., Emerson, C. P., Jr., and Ai, X. (2007) *Dev. Biol.* **311**, 464-477

31. Langsdorf, A., Schumacher, V., Shi, X., Tran, T., Zaia, J., Jain, S., Taglienti, M., Kreidberg, J. A., Fine, A., and Ai, X. (2011) *Glycobiology* **21**, 152-161

32. Schumacher, V. A., Schlotzer-Schrehardt, U., Karumanchi, S. A., Shi, X., Zaia, J., Jeruschke, S., Zhang, D., Pavenstaedt, H., Drenckhan, A., Amann, K., Ng, C., Hartwig, S., Ng, K. H., Ho, J., Kreidberg, J. A., Taglienti, M., Royer-Pokora, B., and Ai, X. (2011) *J. Am. Soc. Nephrol.* **22**, 1286-1296

33. Toyoda, H., Kinoshita-Toyoda, A., and Selleck, S. B. (2000) *J. Biol. Chem.* **275**, 2269-2275

34. Nagamine, S., Keino-Masu, K., Shiomi, K., and Masu, M. (2010) *Biochem. Biophys. Res. Commun.* **391**, 107-112

35. van Kuppevelt, T. H., Dennissen, M. A., van Venrooij, W. J., Hoet, R. M., and Veerkamp, J. H. (1998) *J. Biol. Chem.* **273**, 12960-12966

36. Kurup, S., Wijnhoven, T. J., Jenniskens, G. J., Kimata, K., Habuchi, H., Li, J. P., Lindahl, U., van Kuppevelt, T. H., and Spillmann, D. (2007) *J. Biol. Chem.* **282**, 21032-21042

37. Maccarana, M., Sakura, Y., Tawada, A., Yoshida, K., and Lindahl, U. (1996) *J. Biol. Chem.* **271**, 17804-17810

38. Ledin, J., Staatz, W., Li, J. P., Gotte, M., Selleck, S., Kjellen, L., and Spillmann, D. (2004) *J. Biol. Chem.* **279**, 42732-42741

39. Warda, M., Toida, T., Zhang, F., Sun, P., Munoz, E., Xie, J., and Linhardt, R. J. (2006) *Glycoconj. J.* **23**, 555-563

40. Shi, X., and Zaia, J. (2009) *J. Biol. Chem.* **284**, 11806-11814
41. Ratelade, J., Arrondel, C., Hamard, G., Garbay, S., Harvey, S., Biebuyck, N., Schulz, H., Hastie, N., Pontoglio, M., Gubler, M. C., Antignac, C., and Heidet, L. (2010) *Hum. Mol. Genet.* **19**, 1-15
42. Hossain, M. M., Hosono-Fukao, T., Tang, R., Sugaya, N., van Kuppevelt, T. H., Jenniskens, G. J., Kimata, K., Rosen, S. D., and Uchimura, K. (2010) *Glycobiology* **20**, 175-186
43. Habuchi, H., Habuchi, O., and Kimata, K. (2004) *Glycoconj. J.* **21**, 47-52
44. Tang, R., and Rosen, S. D. (2009) *J. Biol. Chem.* **284**, 21505-21514
45. Jenniskens, G. J., Hafmans, T., Veerkamp, J. H., and van Kuppevelt, T. H. (2002) *Dev. Dyn.* **225**, 70-79
46. Hosono-Fukao, T., Ohtake-Niimi, S., Nishitsuji, K., Hossain, M. M., van Kuppevelt, T. H., Michikawa, M., and Uchimura, K. (2011) *J. Neurosci. Res.* **89**, 1840-1848
47. Lum, D. H., Tan, J., Rosen, S. D., and Werb, Z. (2007) *Mol. Cell Biol.* **27**, 678-688

FOOTNOTES

The abbreviations used are: CS, chondroitin sulfate; GalNAc, *N*-acetylgalactosamine; GlcNAc, *N*-acetylglucosamine; GlcNS, *N*-sulfated glucosamine; HPLC, high performance liquid chromatography; HS, heparan sulfate; PBS, phosphate buffered saline; PFA, paraformaldehyde; RT-PCR, reverse transcriptase-polymerase chain reaction; UA, uronic acid. ΔUA-GlcNAc, 2-acetamido-2-deoxy-4-*O*-(4-deoxy-α-L-*threo*-hex-enepyranosyluronic acid)-D-glucose; ΔUA-GlcNS, 2-deoxy-2-sulfamido-4-*O*-(4-deoxy- α-L-*threo*-hex-enepyranosyluronic acid)-D-glucose; ΔUA-GlcNAc6S, 2-acetamido-2-deoxy-4-*O*-(4-deoxy-α-L-*threo*-hex-enepyranosyluronic acid)-6-*O*-sulfo-D-glucose; ΔUA2S-GlcNAc, 2-acetamido-2-deoxy-4-*O*-(4-deoxy-2-*O*-sulfo-α-L-*threo*-hex-enepyranosyluronic acid)-D-glucose; ΔUA-GlcNS6S, 2-deoxy-2-sulfamido-4-*O*-(4-deoxy- α-L-*threo*-hex-enepyranosyluronic acid)-6-*O*-sulfo-D-glucose; ΔUA2S-GlcNS, 2-deoxy-2-sulfamido-4-*O*-(4-deoxy-2-*O*-sulfo-α-L-*threo*-hex-enepyranosyluronic acid)-D-glucose; ΔUA2S-GlcNAc6S, 2-acetamido-2-deoxy-4-*O*-(4-deoxy-2-*O*-sulfo-α-L-*threo*-hex-enepyranosyluronic acid)-6-*O*-sulfo-D-glucose; ΔUA2S-GlcNS6S, 2-deoxy-2-sulfamido-4-*O*-(4-deoxy-2-*O*-sulfo- α-L-*threo*-hex-enepyranosyluronic acid)-6-*O*-sulfo -D-glucose; ΔDi-0S, 2-acetamido-2-deoxy-3-*O*-(β-D-gluco-4-enepyranosyluronic acid)-D-galactose; ΔDi-4S, 2-acetamido-2-deoxy-3-*O*-(β-D-gluco-4-enepyranosyluronic acid)-4-*O*-sulfo-D-galactose; ΔDi-6S, 2-acetamido-2-deoxy-3-*O*-(β-D-gluco-4-enepyranosyluronic acid)-6-*O*-sulfo-D-galactose; ΔDi-diS$_D$, 2-acetamido-2-deoxy-3-*O*-(2-*O*-sulfo-β-D-gluco-4-enepyranosyluronic acid)-6-*O*-sulfo-D-galactose; ΔDi-diS$_E$, 2-acetamido-2-deoxy-3-*O*-(β-D-gluco-4-enepyranosyluronic acid)-4,6-di-*O*-sulfo-D-galactose; ΔDi-triS, 2-acetamido-2-deoxy-3-*O*-(2-*O*-sulfo-β-D-gluco-4-enepyranosyluronic acid)-4,6-di-*O*-sulfo-D-galactose; ΔDi-HA, 2-acetamido-2-deoxy-3-*O*-(β-D-gluco-4-enepyranosyluronic acid)-D-glucose.

FIGURE LEGENDS
FIGURE 1. Chromatograms of HS unsaturated disaccharides. (A) A chromatogram of 8 standard HS disaccharides. Peak 1, ΔUA-GlcNAc; 2, ΔUA-GlcNS; 3, ΔUA-GlcNAc6S; 4, ΔUA2S-GlcNAc; 5, ΔUA-GlcNS6S; 6, ΔUA2S-GlcNS; 7, ΔUA2S-GlcAc6S; and 8, ΔUA2S-GlcNS6S. The dotted line indicates NaCl concentration. (B) Representative chromatograms of HS disaccharides from 8 organs of wild-type mice. Asterisks indicate peaks of unknown origin. (C) The chromatograms of HS disaccharides from *Sulf1*$^{+/+}$ and *Sulf1*$^{-/-}$ lungs. The *Sulf1*$^{-/-}$ lung contains higher ΔUA2S-GlcNS6S (peak 8) and lower ΔUA2S-GlcNS (peak 6) than those from wild-type controls.

FIGURE 2. Changes in 6-*O*-sulfated HS disaccharide units in *Sulf* knockout mice. Percentages of ΔUA-GlcNAc6S, ΔUA-GlcNS6S, and ΔUA2S-GlcNS6S in total HS of *Sulf1$^{-/-}$* (A) and *Sulf2$^{-/-}$* (B) mice are shown. Abbreviations: Br, brain; Li, liver; In, small intestine; Lu, lung; Ki, kidney; Sp, spleen; Te, testis; Mu, muscle. Bars indicate means ± S.E.M. Statistical significance compared with the wild-type controls (unpaired *t* test; * $P < 0.05$, ** $P < 0.01$, *** $P < 0.001$) is shown. Refer to Tables 1 and 2 for the numbers of mice examined and the values for each disaccharide composition.
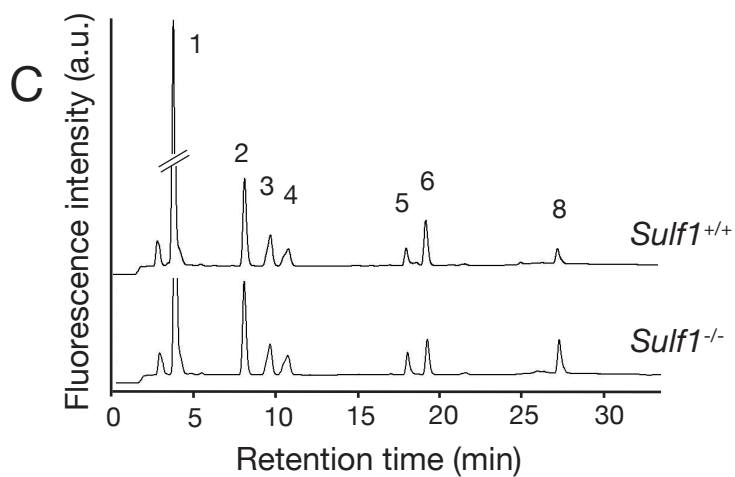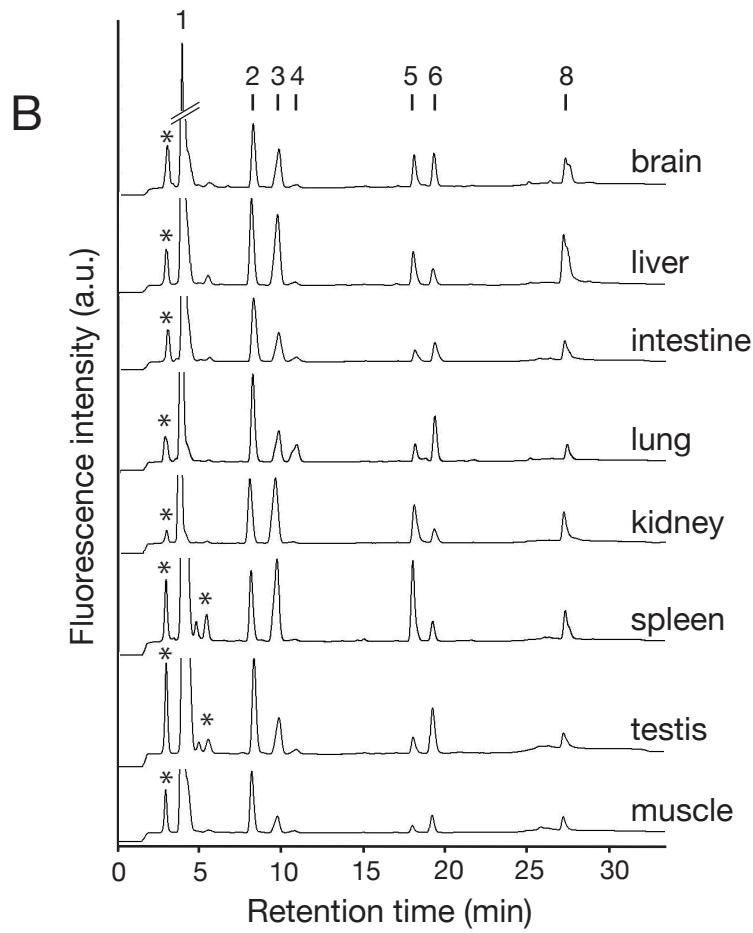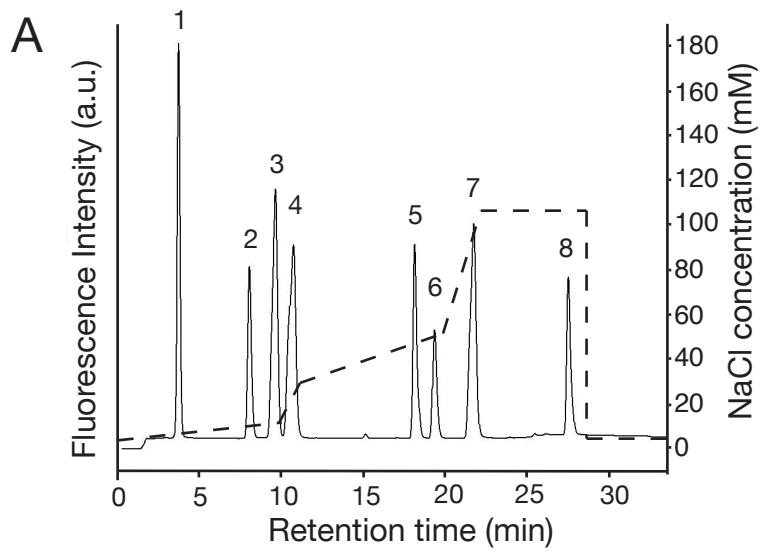
FIGURE 3. Correlation between *Sulf* mRNA expression and changes in HS sulfation patterns in *Sulf* knockout mouse organs. The levels of *Sulf1* or *Sulf2* mRNA expression in 8 organs of wild-type mice were quantitatively determined and normalized to *Gapdh* expression. Increase in ΔUA2S-GlcNS6S in *Sulf1* or *Sulf2* knockout as compared with wild-type controls (%) was calculated. (A) *Sulf1* expression in the wild-type mice and increase in ΔUA2S-GlcNS6S in *Sulf1* knockout mice and (B) *Sulf2* expression in the wild-type mice and increase in ΔUA2S-GlcNS6S in *Sulf2* knockout mice in 8 organs are plotted. The insets show magnifications of the low expression regions. *Sulf1* expression was highly correlated with increase in ΔUA2S-GlcNS6S in *Sulf1* knockout mice ($R = 0.87$).

FIGURE 4. Changes in 6-*O*-sulfated disaccharide units in neonatal *Sulf* knockout mice. (A) Percentages of ΔUA-GlcNAc6S, ΔUA-GlcNS6S, and ΔUA2S-GlcNS6S in total HS and (B) percentages of ΔDi-6S and ΔDi-diS$_E$ in total CS in wild-type, *Sulf1* knockout, *Sulf2* knockout, and *Sulf1/2* double knockout mice are shown. Bars indicate means ± S.E.M. ANOVA with the Bonferroni post hoc test was performed for each organ, and statistical significance compared with the wild-type controls (* $P < 0.05$, ** $P < 0.01$, *** $P < 0.001$) is shown. Refer to Table S1 for the numbers of mice examined and values for each disaccharide composition.
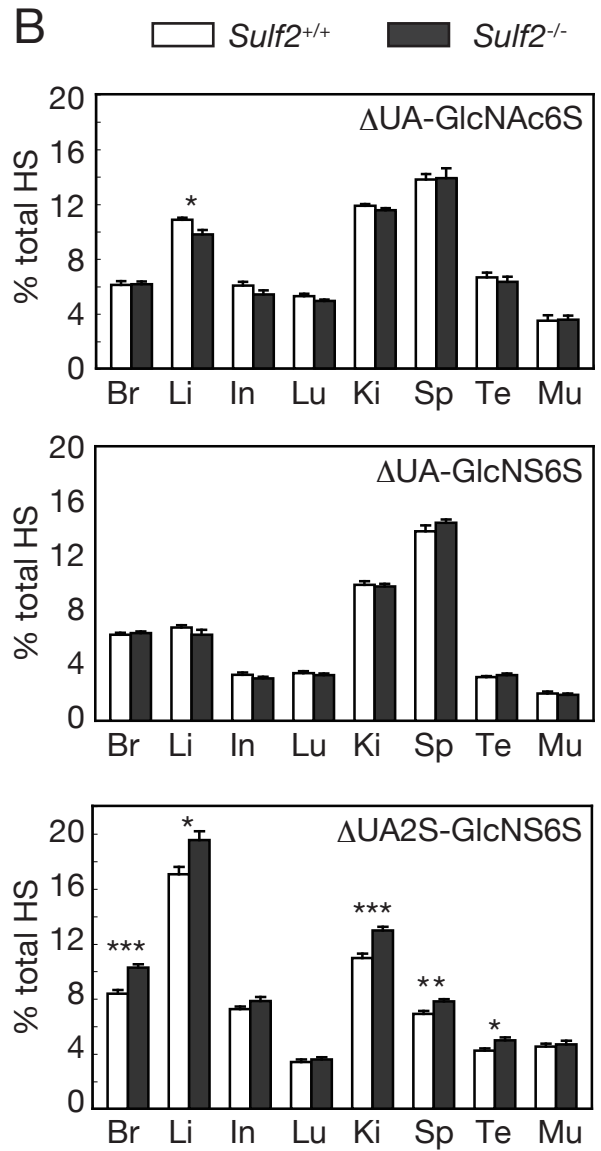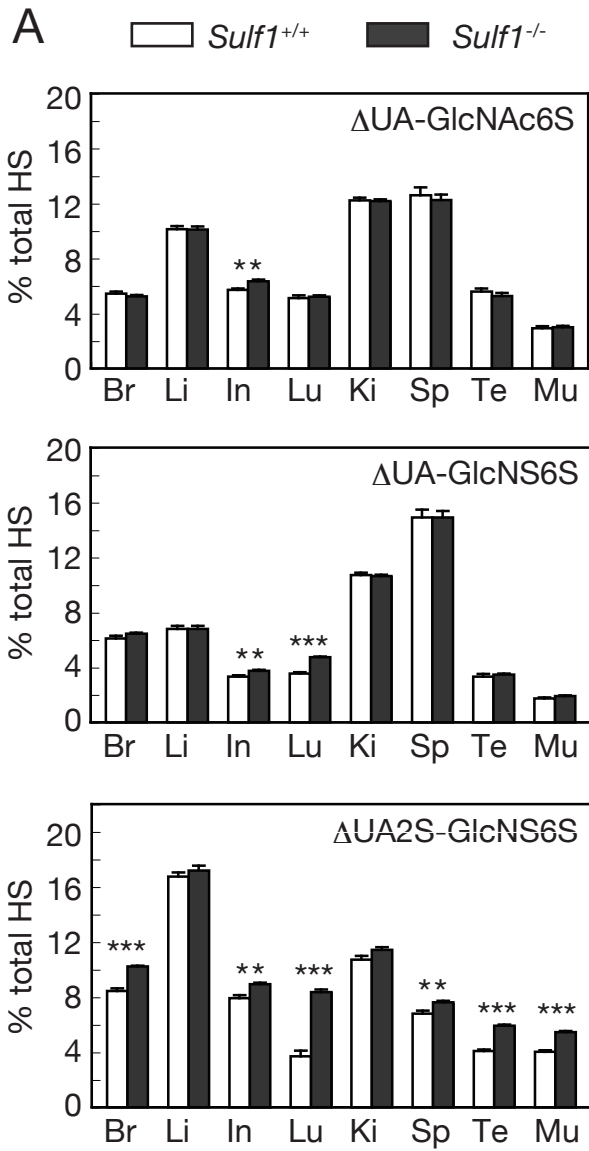
FIGURE 5. *In situ* hybridization of *Sulf1* and *Sulf2*. Cryostat sections of the adult lung (A-B), kidney (C-D), and testis (E-F) were hybridized with digoxigenin-labeled RNA probes specific to *Sulf1* (A, C, E) or *Sulf2* (B, D, F). The signals were detected by BM purple. Arrows in (C) and (D) indicate expression of *Sulf1* in glomeruli and *Sulf2* in distal renal tubules, respectively. Asterisks in (E) and (F) indicate the seminiferous tubules containing Sertoli cells expressing *Sulf1* and *Sulf2*, respectively. Abbreviations: b, bronchus; p, pulmonary artery. Scale bar, 100 μm.

FIGURE 6. Immunohistochemistry of HS in adult kidneys. Cryostat sections of the adult kidneys from wild-type (A, D), *Sulf1$^{-/-}$* (B, E), and *Sulf2$^{-/-}$* (C, F) mice were incubated with anti-HS antibodies RB4CD12 (A-C) or AO4B08 (D-F). The antibody binding was detected by incubation with anti-Myc (A-C) or anti-VSV-G (D-F) antibodies and then by incubation with Alexa568-conjugated anti-rabbit IgG antibody. Asterisks indicate glomeruli. Scale bar, 50 μm.

FIGURE 7. Immunohistochemistry of HS in neonatal lungs. Cryostat sections of the neonatal lungs from wild-type (A, E), *Sulf1$^{-/-}$* (B, F), *Sulf2$^{-/-}$* (C, G), and *Sulf1$^{-/-}$*; *Sulf2$^{-/-}$* (D, H) mice were incubated with anti-HS antibodies RB4CD12 (A-D) or AO4B08 (E-H). The antibody binding was detected by incubation with anti-Myc (A-D) or anti-VSV-G (E-H) antibodies and then by incubation with Alexa568-conjugated anti-rabbit IgG antibody. Abbreviations: b, bronchus; v, blood vessels. Scale bar, 50 μm.

13

Nagamine et al. Figure 1

14

Nagamine et al. Figure 2

A

Increase in ΔUA2S-GlcNS6S (%)

mRNA expression (*Sulf1*/*Gapdh* x 10^5)

(inset) intestine, kidney, liver

lung, testis, muscle, brain, spleen

B

Increase in ΔUA2S-GlcNS6S (%)

mRNA expression (*Sulf2*/*Gapdh* x 10^5)

(inset) kidney, brain, liver, intestine, muscle

brain, spleen, testis, lung

Nagamine et al. Figure 3

16

A

ΔUA-GlcNAc6S

ΔUA-GlcNS6S

ΔUA2S-GlcNS6S

B

ΔDi-6S

ΔDi-diS$_E$

Sulf1$^{+/+}$;Sulf2$^{+/+}$
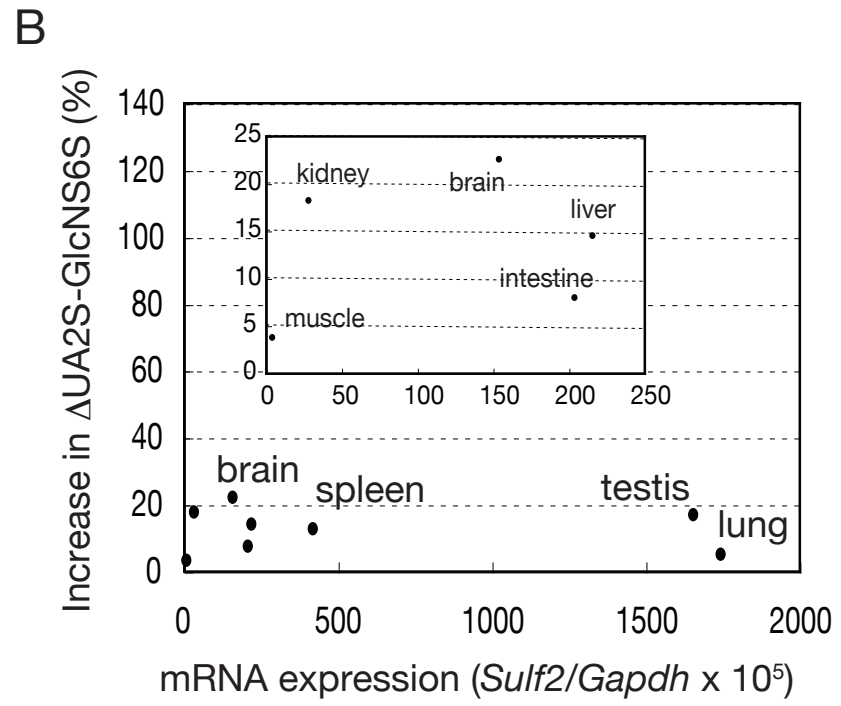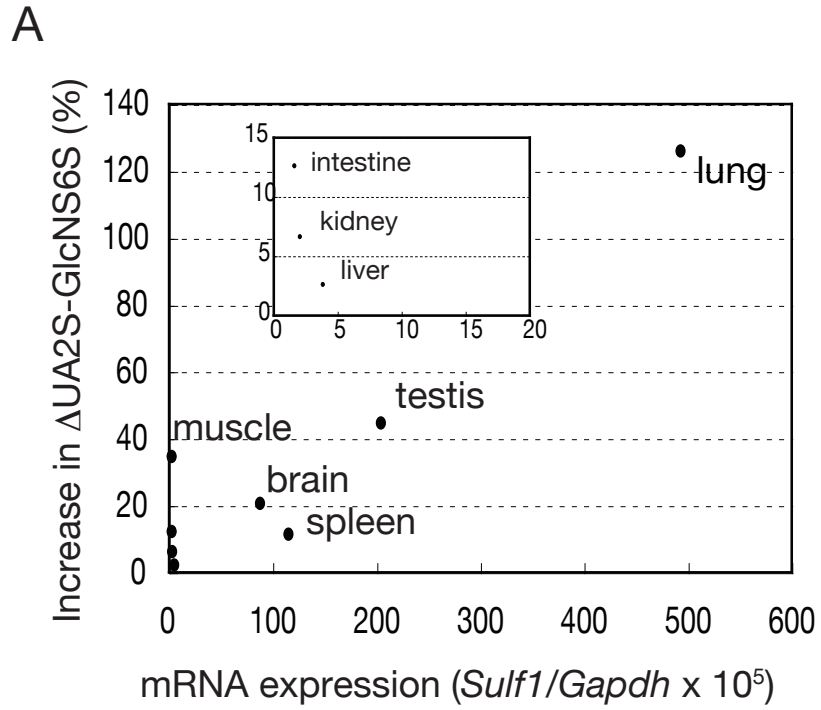
Sulf1$^{-/-}$;Sulf2$^{+/+}$

Sulf1$^{+/+}$;Sulf2$^{-/-}$
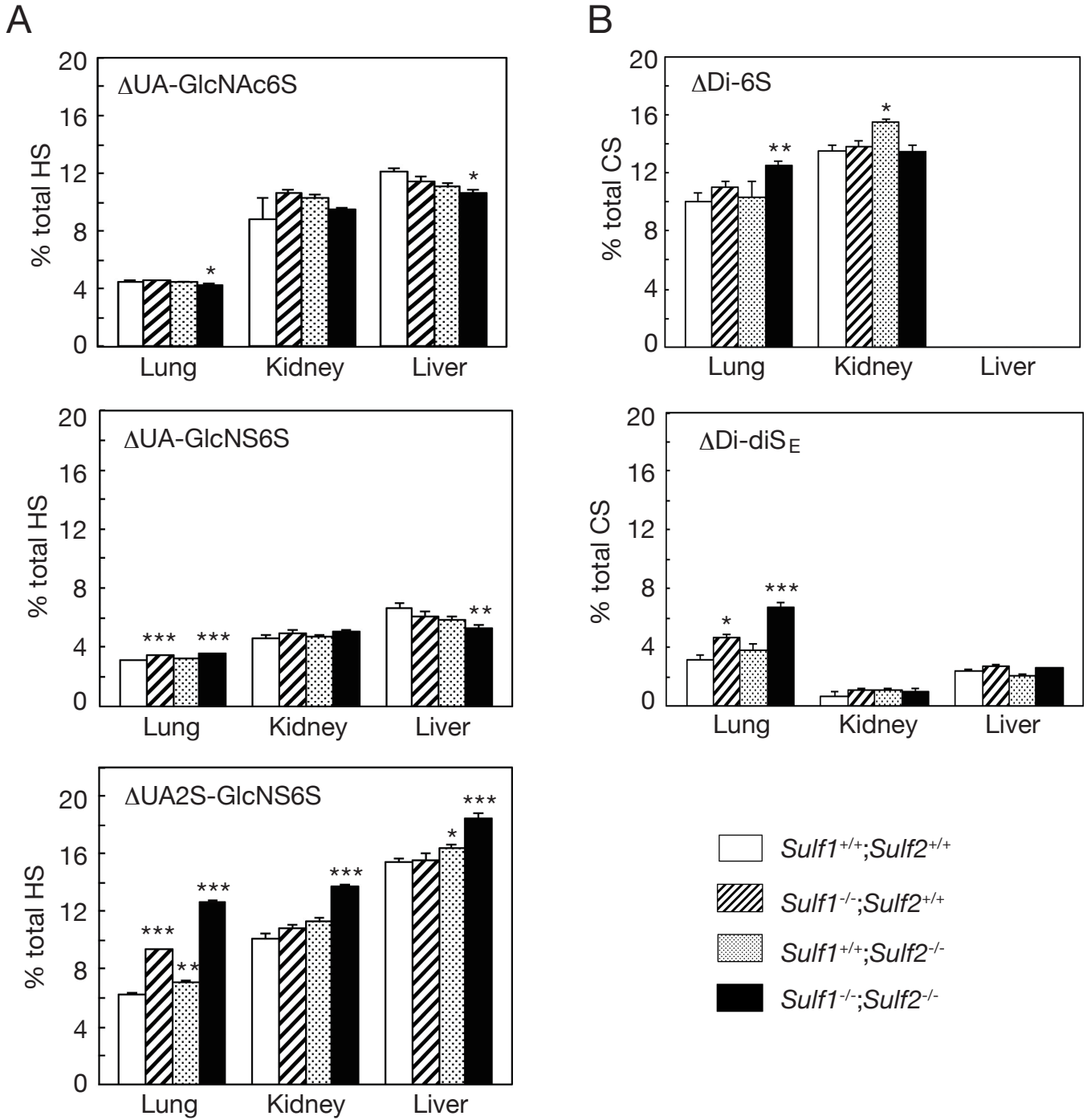
Sulf1$^{-/-}$;Sulf2$^{-/-}$

Nagamine et al. Figure 4

Sulf1   *Sulf2*

Nagamine et al. Figure 5

	Wild-type	*Sulf1*-/-	*Sulf2*-/-

Nagamine et al. Figure 6

| | Wild-type | *Sulf1*^{-/-} | *Sulf2*^{-/-} | *Sulf1*^{-/-};*Sulf2*^{-/-} |

Nagamine et al. Figure 7

20

Table 1. HS disaccharide composition in *Sulf1* knockout mouse organs

Disaccharides	Brain *Sulf1*^{+/+} (n = 6)	Brain *Sulf1*^{-/-} (n = 7)	SA	Liver *Sulf1*^{+/+} (n = 6)	Liver *Sulf1*^{-/-} (n = 7)	SA	Small Intestine *Sulf1*^{+/+} (n = 5)	Small Intestine *Sulf1*^{-/-} (n = 7)	SA	Lung *Sulf1*^{+/+} (n = 5)	Lung *Sulf1*^{-/-} (n = 7)	SA
ΔUA-GlcNAc	46.9 ± 0.77	47.5 ± 0.72		42.5 ± 0.31	42.2 ± 0.13		52.7 ± 0.19	52.2 ± 0.46		45.3 ± 1.26	44.9 ± 0.56	
ΔUA-GlcNS	17.3 ± 0.42	16.7 ± 0.30		17.6 ± 0.14	17.5 ± 0.24		19.9 ± 0.19	19.6 ± 0.19		21.4 ± 0.76	20.3 ± 0.36	
ΔUA-GlcNAc6S	5.4 ± 0.15	5.2 ± 0.10		10.1 ± 0.22	10.1 ± 0.22		5.7 ± 0.10	6.3 ± 0.13	**	5.1 ± 0.20	5.2 ± 0.11	
ΔUA2S-GlcNAc	1.0 ± 0.09	0.9 ± 0.05		0.4 ± 0.02	0.4 ± 0.03		1.0 ± 0.08	0.9 ± 0.05		3.6 ± 0.29	3.3 ± 0.20	
ΔUA-GlcNS6S	6.1 ± 0.20	6.5 ± 0.08		6.8 ± 0.22	6.8 ± 0.22		3.3 ± 0.10	3.7 ± 0.08	**	3.5 ± 0.10	4.7 ± 0.05	***
ΔUA2S-GlcNS	14.7 ± 0.58	12.8 ± 0.42	*	5.8 ± 0.14	5.6 ± 0.29		9.3 ± 0.23	8.3 ± 0.22	**	17.2 ± 0.73	12.8 ± 0.23	** #
ΔUA2S-GlcNAc6S	0.2 ± 0.02	0.2 ± 0.01	*	0.1 ± 0.01	0.1 ± 0.01		0.1 ± 0.01	0.1 ± 0.01		0.3 ± 0.02	0.4 ± 0.01	***
ΔUA2S-GlcNS6S	8.4 ± 0.18	10.2 ± 0.07	***	16.7 ± 0.32	17.2 ± 0.36		7.9 ± 0.23	8.9 ± 0.13	**	3.7 ± 0.43	8.4 ± 0.19	***
N-sulfate	46.5 ± 0.75	46.2 ± 0.66		46.9 ± 0.20	47.2 ± 0.15		40.5 ± 0.15	40.6 ± 0.34		45.8 ± 1.17	46.2 ± 0.43	
2-*O*-sulfate	24.2 ± 0.59	24.1 ± 0.49		23.0 ± 0.22	23.3 ± 0.20		18.3 ± 0.14	18.1 ± 0.25		24.7 ± 0.80	24.8 ± 0.33	
6-*O*-sulfate	20.1 ± 0.51	22.1 ± 0.17	**	33.7 ± 0.48	34.2 ± 0.47		17.0 ± 0.43	19.1 ± 0.29	**	12.6 ± 0.63	18.7 ± 0.29	***

Disaccharides	Kidney *Sulf1*^{+/+} (n = 5)	Kidney *Sulf1*^{-/-} (n = 7)	SA	Spleen *Sulf1*^{+/+} (n = 5)	Spleen *Sulf1*^{-/-} (n = 7)	SA	Testis *Sulf1*^{+/+} (n = 6)	Testis *Sulf1*^{-/-} (n = 7)	SA	Muscle *Sulf1*^{+/+} (n = 6)	Muscle *Sulf1*^{-/-} (n = 7)	SA
ΔUA-GlcNAc	41.4 ± 0.36	41.0 ± 0.40		46.2 ± 1.06	46.6 ± 0.86		52.7 ± 0.42	52.8 ± 0.51		62.9 ± 0.39	62.6 ± 0.44	
ΔUA-GlcNS	18.2 ± 0.07	18.4 ± 0.13		13.8 ± 0.21	13.5 ± 0.17		19.8 ± 0.12	19.5 ± 0.15		18.8 ± 0.13	18.7 ± 0.18	
ΔUA-GlcNAc6S	12.2 ± 0.21	12.2 ± 0.14		12.6 ± 0.57	12.2 ± 0.40		5.6 ± 0.24	5.3 ± 0.22		2.9 ± 0.14	3.0 ± 0.09	
ΔUA2S-GlcNAc	0.2 ± 0.04	0.3 ± 0.03		0.2 ± 0.04	0.3 ± 0.03		0.7 ± 0.03	0.7 ± 0.02		0.7 ± 0.03	0.7 ± 0.04	
ΔUA-GlcNS6S	10.7 ± 0.16	10.7 ± 0.09		14.9 ± 0.57	14.9 ± 0.48		3.3 ± 0.20	3.5 ± 0.07		1.7 ± 0.08	1.9 ± 0.06	
ΔUA2S-GlcNS	6.5 ± 0.21	6.0 ± 0.29		5.3 ± 0.41	4.7 ± 0.16		13.7 ± 0.34	12.2 ± 0.09	** #	8.8 ± 0.16	7.6 ± 0.25	**
ΔUA2S-GlcNAc6S	0.0 ± 0.01	0.1 ± 0.01		0.1 ± 0.04	0.2 ± 0.07		0.0 ± 0.01	0.1 ± 0.01	*	0.1 ± 0.05	0.2 ± 0.06	
ΔUA2S-GlcNS6S	10.7 ± 0.29	11.4 ± 0.20		6.8 ± 0.21	7.6 ± 0.13	**	4.1 ± 0.11	5.9 ± 0.08	***	4.0 ± 0.12	5.4 ± 0.08	***
N-sulfate	46.2 ± 0.42	46.6 ± 0.46		40.9 ± 0.54	40.7 ± 0.46		40.9 ± 0.38	41.1 ± 0.29		33.4 ± 0.30	33.6 ± 0.38	
2-*O*-sulfate	17.5 ± 0.50	17.8 ± 0.42		12.4 ± 0.28	12.7 ± 0.19		18.6 ± 0.32	18.9 ± 0.16		13.6 ± 0.23	13.8 ± 0.34	
6-*O*-sulfate	33.7 ± 0.32	34.3 ± 0.30		34.5 ± 1.21	34.9 ± 0.97		13.0 ± 0.50	14.7 ± 0.33	*	8.9 ± 0.28	10.5 ± 0.16	***

Data are means ± S.E.M. of each disaccharide unit in total HS (%) for each organ. Statistical analysis (SA) done by the Student's *t*-test reveals significant difference between *Sulf1*-deficient mice and the wild-type controls (* $P < 0.05$, ** $P < 0.01$, *** $P < 0.001$). # indicates that Welch's *t*-test was used because 2 groups had unequal variances.

Table 2. HS disaccharide composition in *Sulf2* knockout mouse organs

Disaccharides	Brain $Sulf2^{+/+}$ (n = 6)	Brain $Sulf2^{-/-}$ (n = 6)	SA	Liver $Sulf2^{+/+}$ (n = 7)	Liver $Sulf2^{-/-}$ (n = 6)	SA	Small Intestine $Sulf2^{+/+}$ (n = 7)	Small Intestine $Sulf2^{-/-}$ (n = 7)	SA	Lung $Sulf2^{+/+}$ (n = 7)	Lung $Sulf2^{-/-}$ (n = 7)	SA
ΔUA-GlcNAc	45.3 ± 1.61	44.1 ± 1.49		40.6 ± 1.61	40.9 ± 1.27		53.0 ± 0.97	53.9 ± 1.15		45.3 ± 1.42	42.8 ± 1.38	
ΔUA-GlcNS	17.7 ± 0.57	18.0 ± 0.50		18.2 ± 0.48	18.3 ± 0.43		20.1 ± 0.38	20.2 ± 0.48		21.6 ± 0.80	22.8 ± 0.86	
ΔUA-GlcNAc6S	6.1 ± 0.28	6.1 ± 0.21		10.8 ± 0.16	9.8 ± 0.33	*	6.0 ± 0.28	5.4 ± 0.31		5.3 ± 0.17	4.9 ± 0.09	
ΔUA2S-GlcNAc	1.1 ± 0.11	1.1 ± 0.10		0.4 ± 0.08	0.6 ± 0.09		1.0 ± 0.09	1.0 ± 0.06		3.7 ± 0.34	4.2 ± 0.34	
ΔUA-GlcNS6S	6.3 ± 0.15	6.4 ± 0.11		6.8 ± 0.17	6.3 ± 0.35		3.3 ± 0.18	3.1 ± 0.11		3.5 ± 0.16	3.3 ± 0.12	
ΔUA2S-GlcNS	15.0 ± 0.70	13.9 ± 0.61		6.1 ± 0.26	4.5 ± 0.20	***	9.2 ± 0.21	8.6 ± 0.26		17.1 ± 0.57	18.2 ± 0.49	
ΔUA2S-GlcNAc6S	0.1 ± 0.01	0.1 ± 0.02		0.0 ± 0.01	0.0 ± 0.01		0.0 ± 0.01	0.0 ± 0.01		0.2 ± 0.02	0.2 ± 0.03	
ΔUA2S-GlcNS6S	8.4 ± 0.26	10.2 ± 0.24	***	17.0 ± 0.54	19.5 ± 0.63	*	7.2 ± 0.18	7.8 ± 0.30		3.4 ± 0.18	3.6 ± 0.16	
N-sulfate	47.3 ± 1.34	48.5 ± 1.26		48.1 ± 0.88	48.6 ± 1.03		40.0 ± 0.72	39.7 ± 0.90		45.6 ± 1.28	47.9 ± 1.21	
2-*O*-sulfate	24.6 ± 0.81	25.4 ± 0.79		23.6 ± 0.65	24.7 ± 0.79		17.4 ± 0.32	17.4 ± 0.45		24.4 ± 0.78	26.2 ± 0.71	
6-*O*-sulfate	20.8 ± 0.47	22.9 ± 0.49	*	34.7 ± 0.58	35.6 ± 0.80		16.6 ± 0.57	16.3 ± 0.66		12.3 ± 0.41	12.0 ± 0.26	

Disaccharides	Kidney $Sulf2^{+/+}$ (n = 7)	Kidney $Sulf2^{-/-}$ (n = 7)	SA	Spleen $Sulf2^{+/+}$ (n = 7)	Spleen $Sulf2^{-/-}$ (n = 7)	SA	Testis $Sulf2^{+/+}$ (n = 6)	Testis $Sulf2^{-/-}$ (n = 7)	SA	Muscle $Sulf2^{+/+}$ (n = 7)	Muscle $Sulf2^{-/-}$ (n = 6)	SA
ΔUA-GlcNAc	38.9 ± 0.94	39.6 ± 0.47		44.8 ± 0.71	44.7 ± 1.16		51.2 ± 1.31	51.6 ± 1.13		60.3 ± 1.50	60.1 ± 1.08	
ΔUA-GlcNS	19.1 ± 0.27	19.2 ± 0.28		14.7 ± 0.49	14.7 ± 0.57		20.6 ± 0.63	20.3 ± 0.40		19.5 ± 0.53	19.6 ± 0.45	
ΔUA-GlcNAc6S	11.9 ± 0.12	11.5 ± 0.16		13.8 ± 0.40	13.9 ± 0.72		6.7 ± 0.35	6.3 ± 0.39		3.5 ± 0.40	3.6 ± 0.29	
ΔUA2S-GlcNAc	0.6 ± 0.10	0.6 ± 0.10		0.2 ± 0.05	0.2 ± 0.04		0.7 ± 0.09	0.7 ± 0.04		0.7 ± 0.19	0.7 ± 0.04	
ΔUA-GlcNS6S	9.9 ± 0.25	9.8 ± 0.19		13.8 ± 0.43	14.4 ± 0.25		3.2 ± 0.07	3.3 ± 0.12		2.0 ± 0.16	1.9 ± 0.10	
ΔUA2S-GlcNS	8.7 ± 0.38	6.4 ± 0.27	***	5.8 ± 0.18	4.3 ± 0.26	***	13.4 ± 0.35	12.7 ± 0.38		9.5 ± 0.26	9.5 ± 0.26	
ΔUA2S-GlcNAc6S	0.1 ± 0.02	0.1 ± 0.02		0.0 ± 0.02	0.0 ± 0.01		0.0 ± 0.02	0.0 ± 0.02		0.0 ± 0.02	0.0 ± 0.01	#
ΔUA2S-GlcNS6S	10.9 ± 0.33	12.9 ± 0.27	***	6.9 ± 0.21	7.8 ± 0.16	**	4.2 ± 0.16	5.0 ± 0.20	*	4.5 ± 0.23	4.7 ± 0.26	
N-sulfate	48.6 ± 0.89	48.2 ± 0.49		41.2 ± 0.45	41.2 ± 0.59		40.6 ± 1.19	41.3 ± 0.78		35.4 ± 1.46	35.7 ± 0.80	
2-*O*-sulfate	20.3 ± 0.76	20.0 ± 0.48		12.9 ± 0.26	12.3 ± 0.22		17.4 ± 0.99	18.4 ± 0.44		14.8 ± 0.47	14.9 ± 0.35	
6-*O*-sulfate	32.8 ± 0.41	34.3 ± 0.34	*	34.5 ± 0.61	36.1 ± 0.90		13.9 ± 0.40	14.6 ± 0.66		10.0 ± 0.97	10.2 ± 0.41	

Data are means ± S.E.M. of each disaccharide unit in total HS (%) for each organ. Statistical analysis (SA) done by the Student's *t*-test reveals significant difference between *Sulf2*-deficient mice and the wild-type controls (* $P < 0.05$, ** $P < 0.01$, *** $P < 0.001$). # indicates that Welch's *t*-test was used because 2 groups had unequal variances.

Table 3. HS and CS disaccharide composition in *Sulf1/Sulf2* knockout neonatal mouse organs

	Lung (n = 6)				Kidney (n = 3)				Liver (n = 6)			
HS Disaccharides	*Sulf1*$^{+/+}$;*Sulf2*$^{+/+}$	*Sulf1*$^{-/-}$;*Sulf2*$^{+/+}$	*Sulf1*$^{+/+}$;*Sulf2*$^{-/-}$	*Sulf1*$^{-/-}$;*Sulf2*$^{-/-}$	*Sulf1*$^{+/+}$;*Sulf2*$^{+/+}$	*Sulf1*$^{-/-}$;*Sulf2*$^{+/+}$	*Sulf1*$^{+/+}$;*Sulf2*$^{-/-}$	*Sulf1*$^{-/-}$;*Sulf2*$^{-/-}$	*Sulf1*$^{+/+}$;*Sulf2*$^{+/+}$	*Sulf1*$^{-/-}$;*Sulf2*$^{+/+}$	*Sulf1*$^{+/+}$;*Sulf2*$^{-/-}$	*Sulf1*$^{-/-}$;*Sulf2*$^{-/-}$
ΔUA-GlcNAc	49.9 ± 0.29	49.2 ± 0.41	49.1 ± 0.22	50.3 ± 0.12	50.6 ± 2.92	47.5 ± 0.42	48.2 ± 0.20	48.2 ± 0.29	43.8 ± 0.53	44.7 ± 0.29	44.5 ± 0.59	44.9 ± 0.33
ΔUA-GlcNS	21.4 ± 0.11	21.0 ± 0.20	21.1 ± 0.05	20.2 ± 0.08 ***	20.8 ± 0.61	21.4 ± 0.26	21.1 ± 0.17	20.6 ± 0.10	17.4 ± 0.17	18.1 ± 0.26 *	18.1 ± 0.14	18.1 ± 0.12
ΔUA-GlcNAc6S	4.5 ± 0.04	4.6 ± 0.06	4.5 ± 0.02	4.3 ± 0.07 *	8.8 ± 1.45	10.7 ± 0.15	10.3 ± 0.17	9.5 ± 0.16	12.1 ± 0.27	11.4 ± 0.38	11.1 ± 0.26	10.6 ± 0.21 *
ΔUA2S-GlcNAc	2.4 ± 0.07	2.3 ± 0.02	2.4 ± 0.05	2.3 ± 0.02	0.0 ± 0.00	0.0 ± 0.00	0.0 ± 0.00	0.0 ± 0.00 *	0.0 ± 0.00	0.0 ± 0.00	0.0 ± 0.00	0.0 ± 0.00
ΔUA-GlcNS6S	3.1 ± 0.03	3.5 ± 0.06 ***	3.2 ± 0.02	3.5 ± 0.02 ***	4.7 ± 0.21	4.9 ± 0.22	4.7 ± 0.11	5.0 ± 0.14	6.7 ± 0.29	6.0 ± 0.33	5.9 ± 0.19	5.3 ± 0.18 **
ΔUA2S-GlcNS	12.3 ± 0.17	9.9 ± 0.10 ***	12.6 ± 0.13	6.6 ± 0.08 ***	5.0 ± 0.34	4.7 ± 0.36	4.3 ± 0.27	3.0 ± 0.10 **	4.5 ± 0.16	4.2 ± 0.18	4.1 ± 0.21	2.5 ± 0.23 ***
ΔUA2S-GlcNAc6S	0.1 ± 0.01	0.2 ± 0.01	0.1 ± 0.01	0.1 ± 0.01	0.0 ± 0.00	0.0 ± 0.00	0.0 ± 0.00	0.0 ± 0.00	0.0 ± 0.00	0.0 ± 0.00	0.0 ± 0.00	0.0 ± 0.00
ΔUA2S-GlcNS6S	6.3 ± 0.08	9.4 ± 0.09 ***	7.0 ± 0.15 **	12.6 ± 0.15 ***	10.1 ± 0.34	10.8 ± 0.22	11.3 ± 0.27	13.7 ± 0.14 ***	15.4 ± 0.18	15.5 ± 0.53	16.3 ± 0.36	18.5 ± 0.34 ***
N-sulfate	43.1 ± 0.19	43.7 ± 0.36	43.9 ± 0.19	43.0 ± 0.06	40.6 ± 1.48	41.8 ± 0.55	41.4 ± 0.22	42.3 ± 0.25	44.1 ± 0.34	43.9 ± 0.28	44.4 ± 0.42	44.4 ± 0.45
2-*O*-sulfate	21.1 ± 0.28	21.7 ± 0.16	22.1 ± 0.22 *	21.6 ± 0.09	15.1 ± 0.67	15.5 ± 0.58	15.5 ± 0.32	16.8 ± 0.12	20.0 ± 0.24	19.8 ± 0.41	20.4 ± 0.46	21.0 ± 0.47
6-*O*-sulfate	14.0 ± 0.10	17.6 ± 0.18 ***	14.9 ± 0.15 **	20.7 ± 0.20 ***	23.6 ± 2.01	26.4 ± 0.27	26.3 ± 0.49	28.2 ± 0.40	34.2 ± 0.57	33.0 ± 0.49	33.4 ± 0.52	34.5 ± 0.24

	Lung (n = 6)				Kidney (n = 3)				Liver (n = 6)			
CS Disaccharides	*Sulf1*$^{+/+}$;*Sulf2*$^{+/+}$	*Sulf1*$^{-/-}$;*Sulf2*$^{+/+}$	*Sulf1*$^{+/+}$;*Sulf2*$^{-/-}$	*Sulf1*$^{-/-}$;*Sulf2*$^{-/-}$	*Sulf1*$^{+/+}$;*Sulf2*$^{+/+}$	*Sulf1*$^{-/-}$;*Sulf2*$^{+/+}$	*Sulf1*$^{+/+}$;*Sulf2*$^{-/-}$	*Sulf1*$^{-/-}$;*Sulf2*$^{-/-}$	*Sulf1*$^{+/+}$;*Sulf2*$^{+/+}$	*Sulf1*$^{-/-}$;*Sulf2*$^{+/+}$	*Sulf1*$^{+/+}$;*Sulf2*$^{-/-}$	*Sulf1*$^{-/-}$;*Sulf2*$^{-/-}$
ΔDi-0S + ΔDi-HA	37.0 ± 2.0	40.6 ± 2.8	35.6 ± 1.8	39.1 ± 0.3	55.4 ± 1.5	53.7 ± 1.6	51.3 ± 0.7	55.9 ± 1.4	32.7 ± 1.6	32.8 ± 1.2	31.1 ± 1.1	31.2 ± 0.5
ΔDi-4S	49.5 ± 2.5	43.3 ± 3.0	50.0 ± 3.1	41.2 ± 0.4 *	30.3 ± 0.9	31.1 ± 1.0	31.8 ± 0.5	29.5 ± 0.8	64.9 ± 1.7	64.4 ± 1.3	66.9 ± 1.2	66.2 ± 0.5
ΔDi-6S	10.0 ± 0.6	11.0 ± 0.4	10.3 ± 1.1	12.5 ± 0.3 **	13.5 ± 0.4	13.8 ± 0.4	15.5 ± 0.3 *	13.5 ± 0.4	0.0 ± 0.0	0.0 ± 0.0	0.0 ± 0.0	0.0 ± 0.0
ΔDi-diS$_E$	3.2 ± 0.2	4.7 ± 0.2 *	3.8 ± 0.5	6.7 ± 0.4 ***	0.7 ± 0.3	1.1 ± 0.1	1.1 ± 0.1	1.0 ± 0.2	2.4 ± 0.1	2.7 ± 0.2	2.0 ± 0.1	2.6 ± 0.2
ΔDi-diS$_D$	0.3 ± 0.0	0.3 ± 0.0	0.3 ± 0.0	0.4 ± 0.0 ***	0.2 ± 0.1	0.2 ± 0.0	0.3 ± 0.0	0.1 ± 0.1	0.0 ± 0.0	0.1 ± 0.1	0.0 ± 0.0	0.0 ± 0.0
ΔDi-triS	0.0 ± 0.0	0.0 ± 0.0	0.0 ± 0.0	0.0 ± 0.0	0.0 ± 0.0	0.0 ± 0.0	0.0 ± 0.0	0.0 ± 0.0	0.0 ± 0.0	0.0 ± 0.0	0.0 ± 0.0	0.0 ± 0.0

Data are means ± S.E.M. of each disaccharide unit in total HS or CS (%) for each organ. Statistical analysis done by ANOVA with Bonferroni post hoc test reveals significant difference between *Sulf/Sulf2* knockout mice and the wild-type controls (* $P < 0.05$, ** $P < 0.01$, *** $P < 0.001$).

SUPPLEMENTAL DATA

EXPERIMENTAL PROCEDURES

Immunohistochemistry—Cryostat sections (5 μm) of snap-frozen kidneys were incubated with anti-HS antibody AO4B08 (1:50) in PBS containing 1% BSA and 5% normal goat serum at room temperature for 60 min. After washing, the sections were incubated with anti-VSV-G antibody (1:500; Rockland Immunochemicals, Gilbertsville, PA, USA) for 60 min. Finally, the slides were incubated with Alexa488-conjugated anti-rabbit IgG (1:200; Invitrogen, Carlsbad, CA, USA) for 60 min and mounted with coverslips using Mowiol. The images were obtained by microscopy (DM6000B; Leica, Wetzler, Germany). Pictures were shot with the same exposure time for comparison.

FIGURE LEGENDS

FIGURE S1. (A, D) Scheme of the targeting strategy for *Sulf1* and *Sulf2*. A stop-*IRES-lacZ-polyA-pgk-Neo* cassette was inserted into exon 5 of *Sulf1* and *Sulf2* genes. DTA, diphtheria toxin A fragment; E, *Eco*RI; K, *Kpn*I; (K), a polymorphic *Kpn*I site present in the 129 (targeted) allele but not in the C57BL/6 (wild-type) allele. (B, E) Southern blots for *Sulf1* (B) and *Sulf2* (E). Genomic DNAs were digested with the indicated restriction enzymes and hybridized with the indicated probes. Closed and open triangles indicate wild-type and targeted alleles, respectively. The sizes of the wild-type and targeted alleles, respectively, are as follows: 12.7 and 10.4 kb for 5' probe, and 7.7 and 5.5 kb for 3' probe in *Sulf1*; and 12.0 and 5.5 kb for 5' probe, and 12.0 and 3.5 kb for 3' probe in *Sulf2*. (C, F) Northern blots indicated that *Sulf1* mRNA expression was abolished whereas *Sulf2* mRNA was not affected in *Sulf1*$^{-/-}$ mice and that *Sulf2* mRNA was abolished whereas *Sulf1* mRNA was not affected in *Sulf2*$^{-/-}$ mice.

FIGURE S2. Chromatograms of CS unsaturated disaccharides. (A) Chromatogram of 6 standard CS disaccharides. Peak 1, ΔDi-0S; 2, ΔDi-4S; 3, ΔDi-6S; 4, ΔDi-diS$_E$; 5, ΔDi-diS$_D$; 6, ΔDi-triS. The dotted line indicates NaCl concentration. (B) Representative chromatograms of CS disaccharides from 8 organs of wild-type mice. Peak 1 in (B) contains ΔDi-0S and ΔDi-HA.

FIGURE S3. Quantitative RT-PCR of *Sulf1* and *Sulf2* mRNA in *Sulf* knockout mice. *Sulf1* and *Sulf2* mRNA expressions in 8 organs of *Sulf* knockout mice were quantitatively determined and normalized to the wild-type control. Sample 1, *Sulf1*$^{+/+}$;*Sulf2*$^{+/+}$; 2, *Sulf1*$^{+/-}$;*Sulf2*$^{+/+}$; 3, *Sulf1*$^{-/-}$;*Sulf2*$^{+/+}$; 4, *Sulf1*$^{+/+}$;*Sulf2*$^{+/-}$; 5, *Sulf1*$^{+/+}$;*Sulf2*$^{-/-}$.

FIGURE S4. Endosulfatase assay. CS-D (A) or CS-E (B) was incubated with conditioned medium from 293EBNA cells transfected with *Sulf1*, *Sulf2*, or control expression plasmids and subsequently digested with chondroitinase ABC and chondroitinase ACII. The resultant disaccharides were analyzed by HPLC. The sulfation patterns of CS-D and CS-E were unchanged after treatment with Sulf1 or Sulf2.

FIGURE S5. *In situ* hybridization of *Sulf1* and *Sulf2* in the adult kidney. Strong *Sulf1* signals were detected in the glomeruli (A, C; arrows), whereas only marginal or weak *Sulf2* signals were detectable in the glomeruli (B, D; arrows). *Sulf1* signals were also seen in the blood vessels (E; arrows). Scale bar, 50 μm.

FIGURE S6. Immunohistochemistry of HS in adult kidneys. Cryostat sections of the adult kidneys from wild-type (A, D), *Sulf1*$^{-/-}$ (B, E), and *Sulf2*$^{-/-}$ (C, F) mice were incubated with anti-HS antibodies, AO4B08 (A-C), or RB4CD12 (D-F). The antibody binding was detected by incubation with anti-VSV-G (A-C) or anti-Myc (D-F) antibodies and then by incubation with Alexa568-conjugated anti-rabbit IgG antibody. Asterisks indicate glomeruli. Scale bar, 50 μm.

FIGURE S7. Immunohistochemistry of HS in adult kidneys. Cryostat sections of the adult kidneys from wild-type (A) and *Sulf1*$^{-/-}$ (B) mice were incubated with AO4B08 diluted at 1:50. The antibody binding was detected by incubation with anti-VSV-G antibody and then by incubation with Alexa488-conjugated anti-rabbit IgG antibody. Positive staining in the blood vessels (v) was observed. Scale bar, 100 μm.

FIGURE S8. Immunohistochemistry of HS in adult lungs. Cryostat sections of the adult lungs from wild-type (A, C) and *Sulf1*$^{-/-}$ (B, D) mice were incubated with anti-HS antibodies RB4CD12 (A-B), or AO4B08 (C-D). The antibody binding was detected by incubation with anti-Myc (A-B) or anti-VSV-G (C-D) antibodies and then by incubation with Alexa568-conjugated anti-rabbit IgG antibody. Abbreviations: b, bronchus; v, blood vessels. Scale bar, 50 μm.

FIGURE S9. Immunohistochemistry of HS in neonatal kidneys. Cryostat sections of the neonatal kidneys from wild-type (A, E), *Sulf1*$^{-/-}$ (B, F), *Sulf2*$^{-/-}$ (C, G), and *Sulf1*$^{-/-}$; *Sulf2*$^{-/-}$ (D, H)

mice were incubated with anti-HS antibodies, RB4CD12 (A-D) or AO4B08 (E-H). The antibody binding was detected by incubation with anti-Myc (A-D) or anti-VSV-G (E-H) antibodies and then by incubation with Alexa568-conjugated anti-rabbit IgG antibody. Arrows indicate glomeruli. Scale bar, 50 μm.
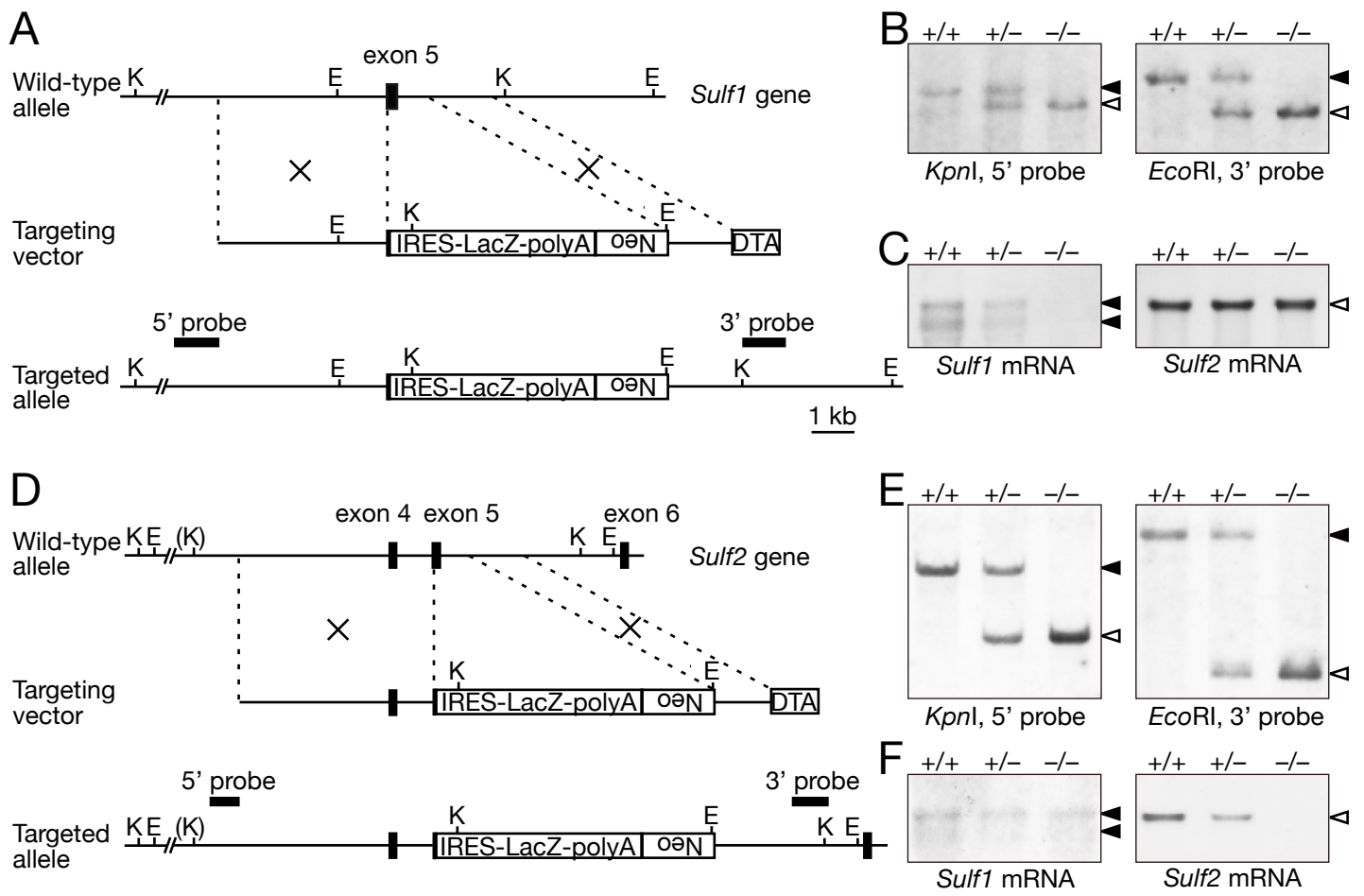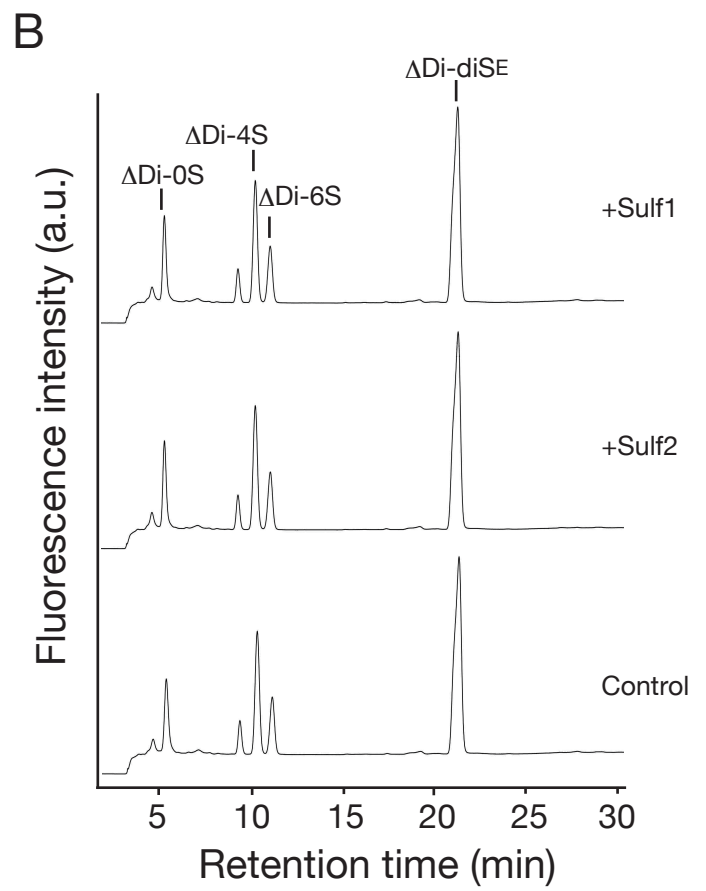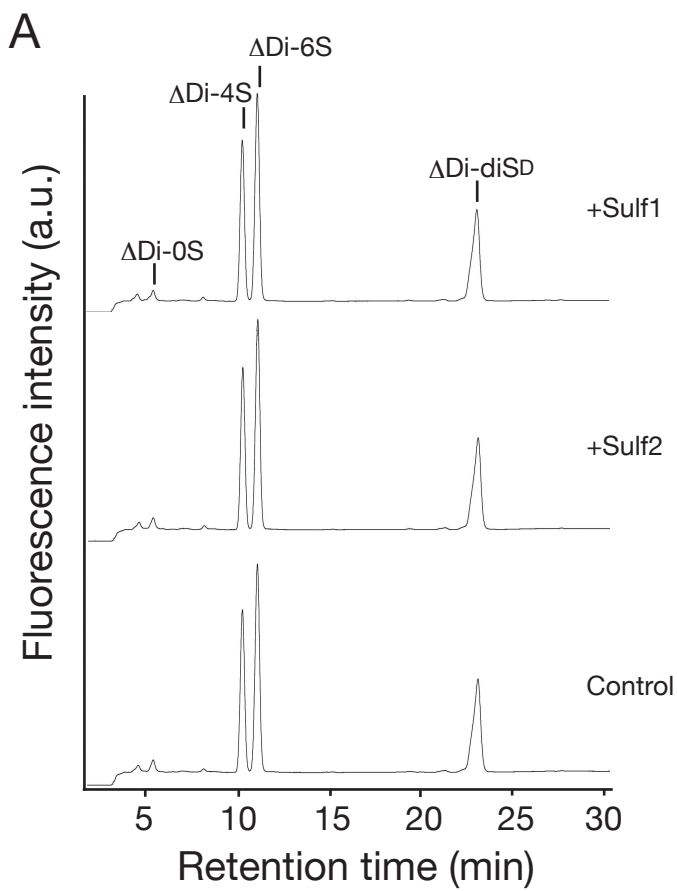
Nagamine et al. Figure S1
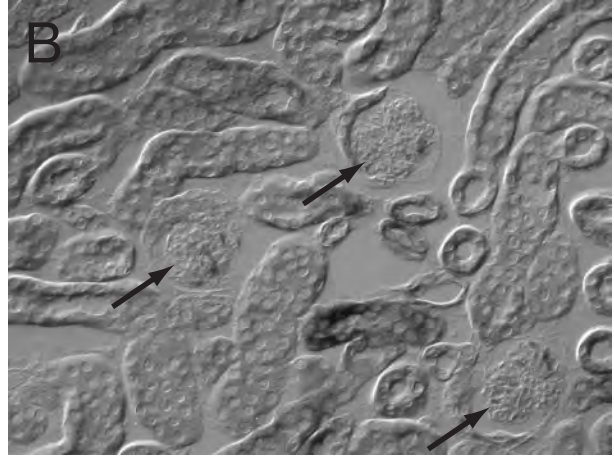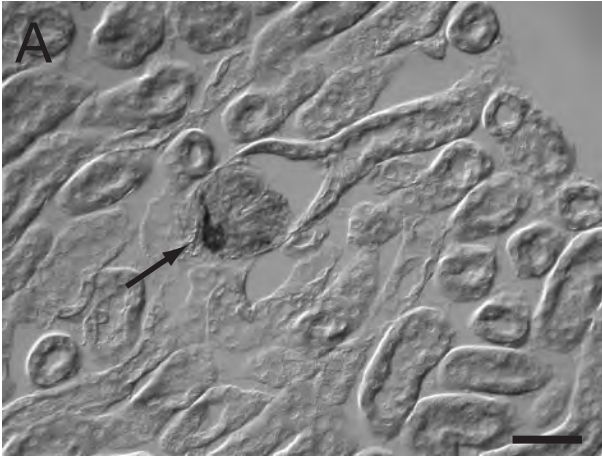
Nagamine et al. Figure S2
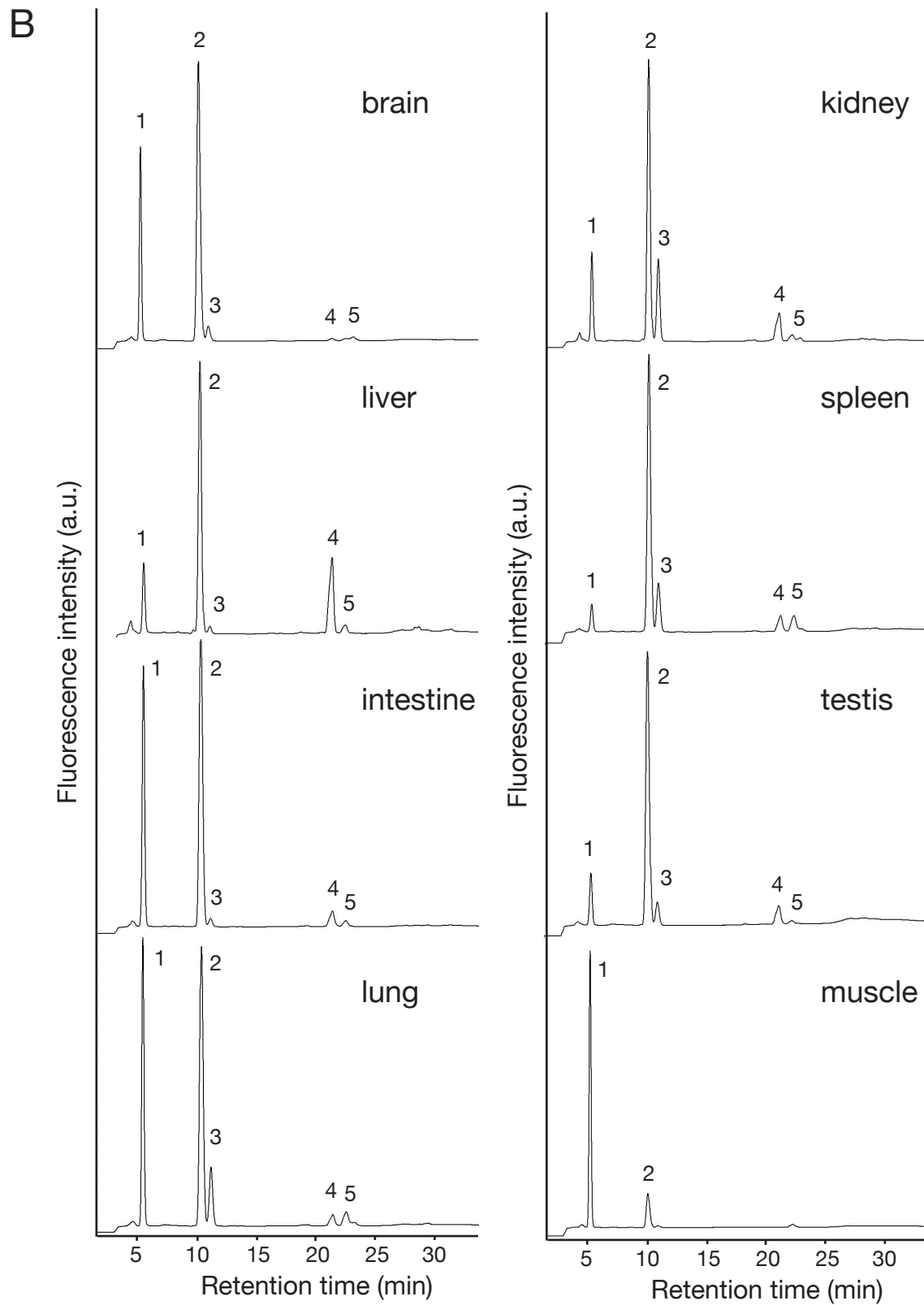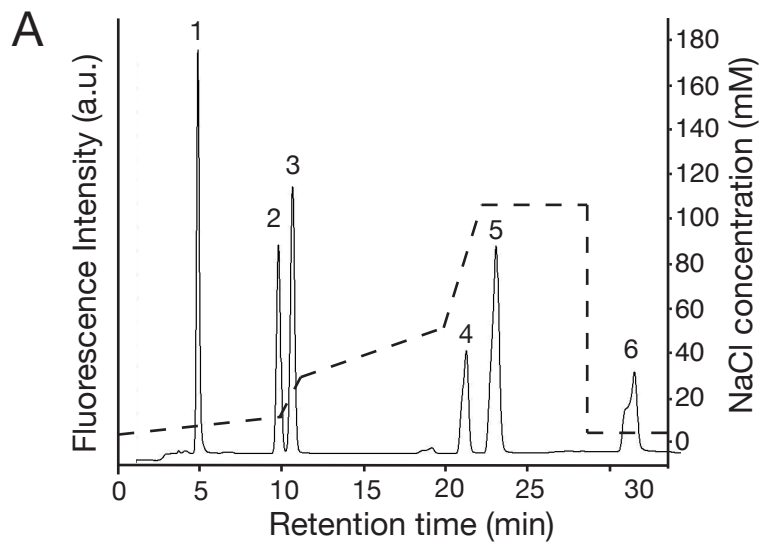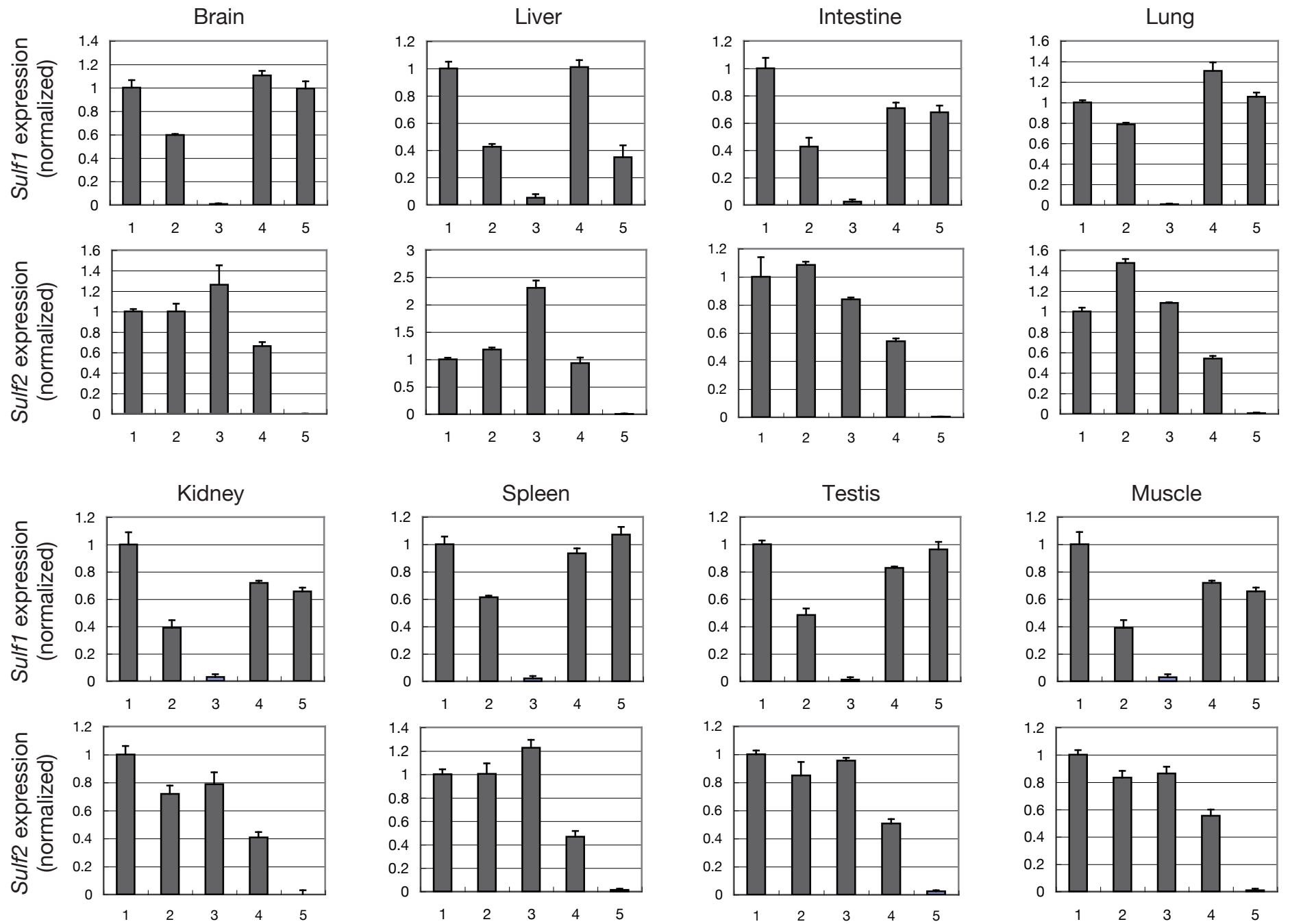
Nagamine et al. Figure S3

Nagamine et al. Figure S4

Sulf1   *Sulf2*

Nagamine et al. Figure S5
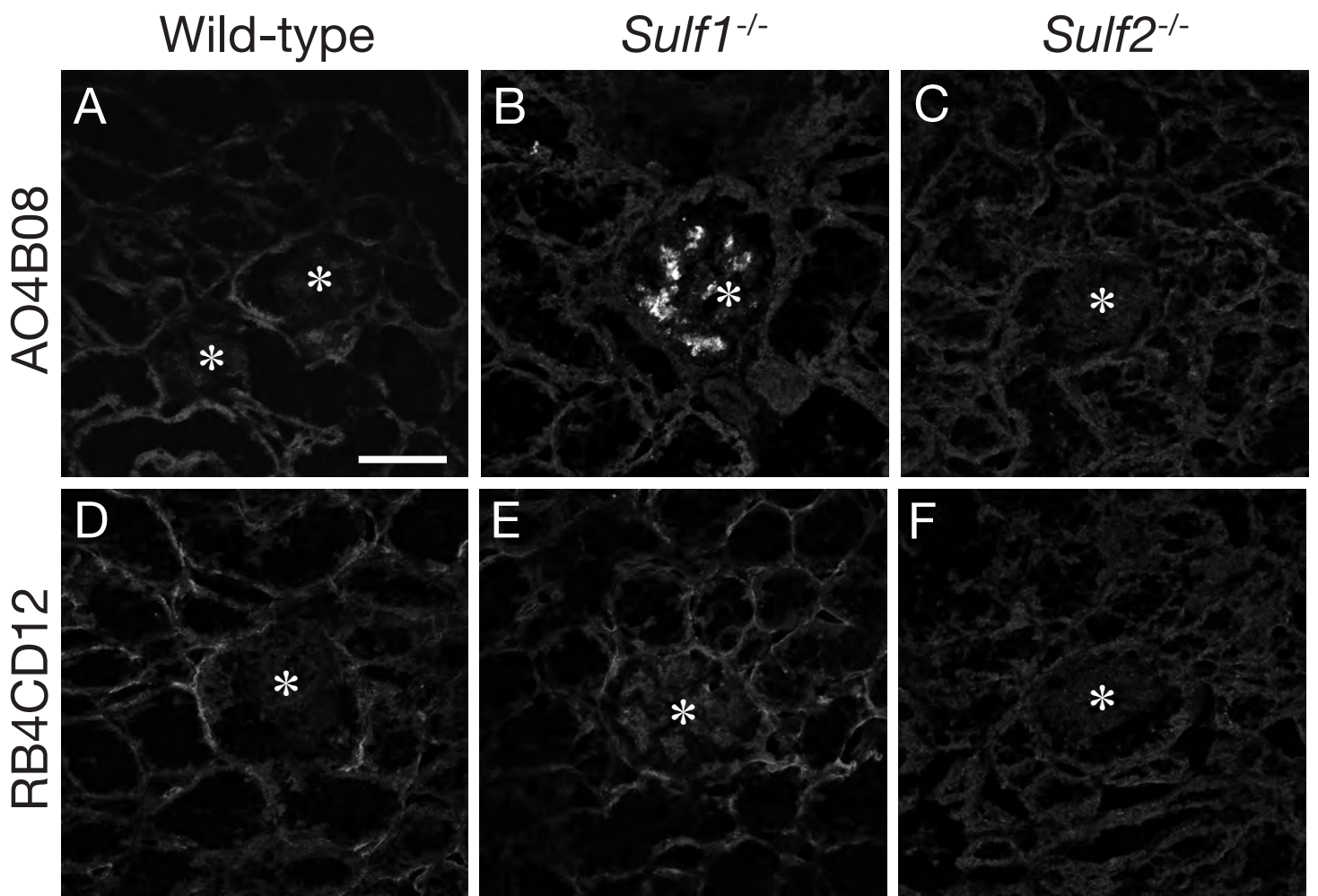
Wild-type *Sulf1^{-/-}* *Sulf2^{-/-}*

AO4B08

RB4CD12

Nagamine et al. Figure S6

Wild-type   *Sulf1*$^{-/-}$

AO4B08

A

B

v

v

100 µm

Nagamine et al. Figure S7

| | Wild-type | *Sulf1*^{-/-} |

Nagamine et al. Figure S8

| | Wild-type | *Sulf1*⁻/⁻ | *Sulf2*⁻/⁻ | *Sulf1*⁻/⁻;*Sulf2*⁻/⁻ |
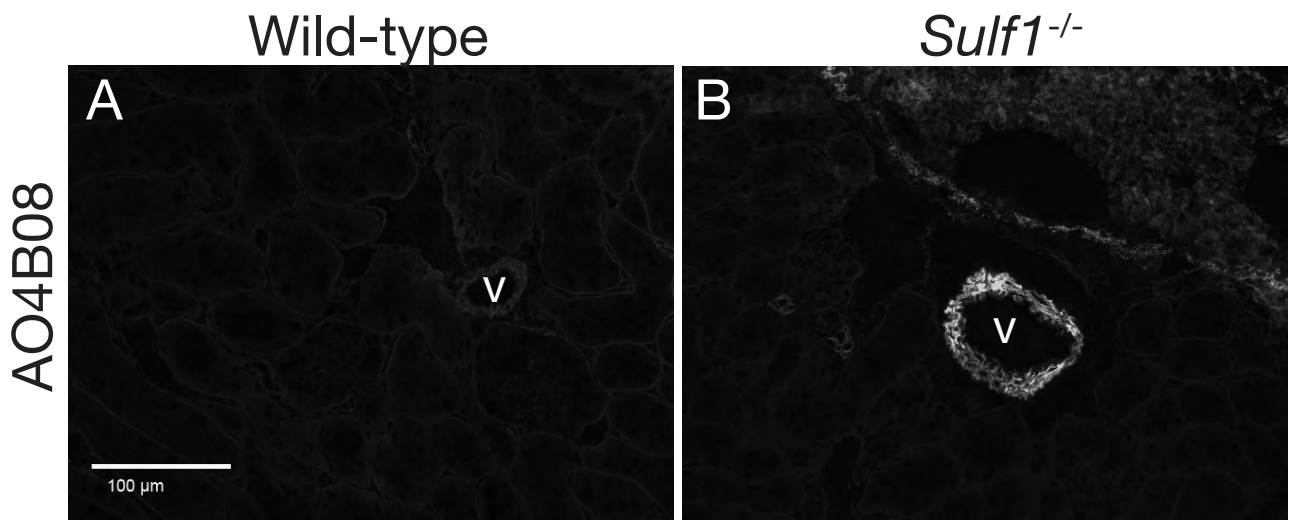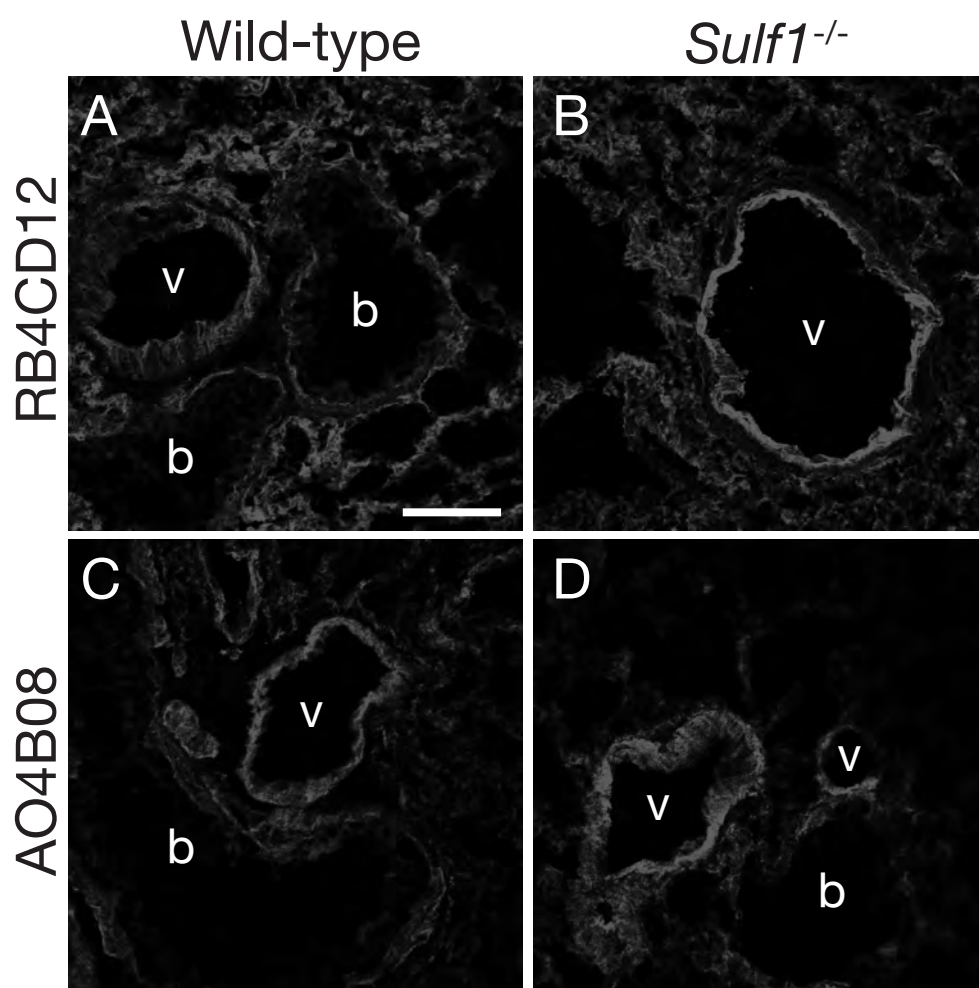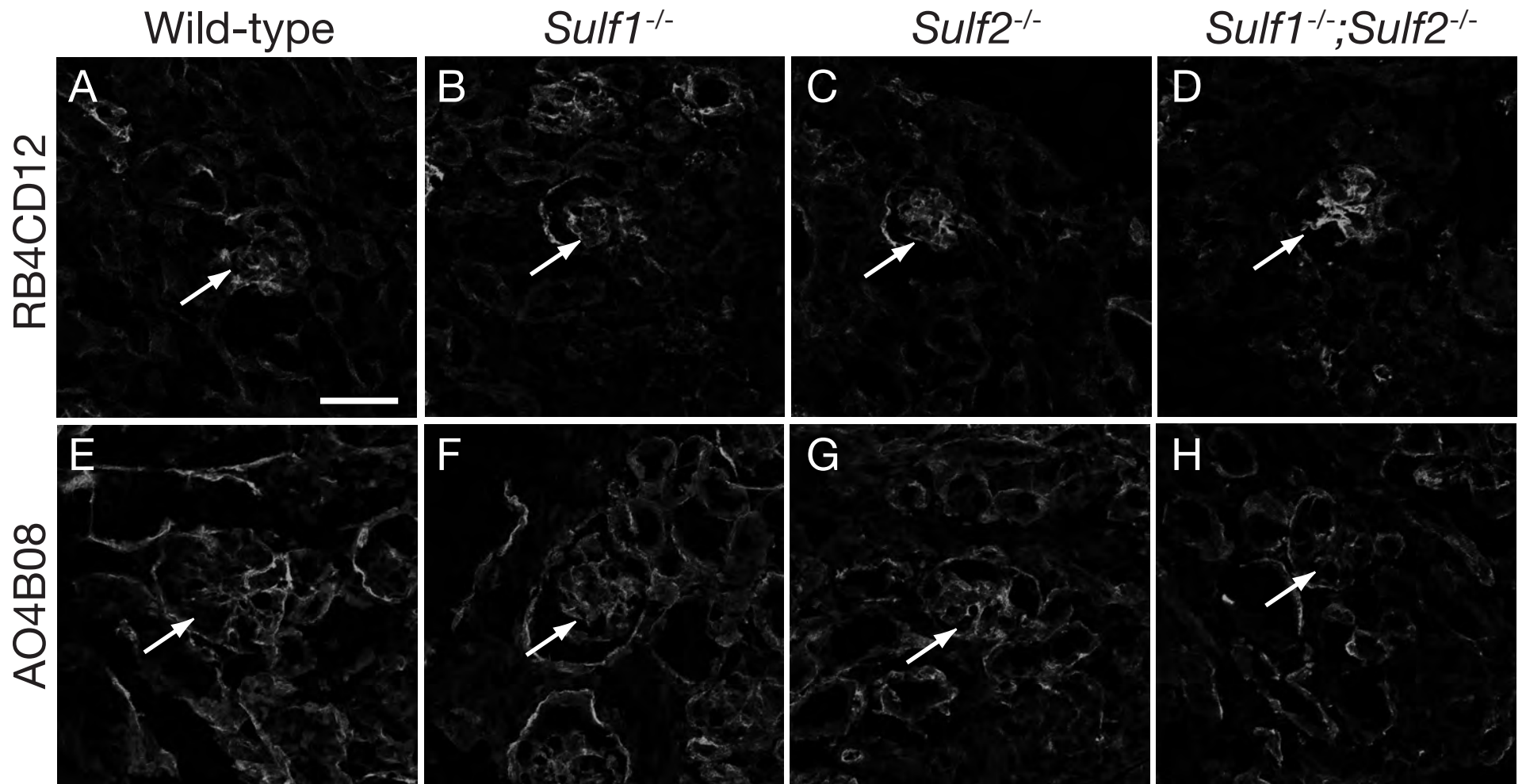
Nagamine et al. Figure S9

Table S1. CS disaccharide composition in *Sulf1* knockout mouse organs

Disaccharides	Brain Sulf1$^{+/+}$ (n = 6)	Brain Sulf1$^{-/-}$ (n = 7)	SA	Liver Sulf1$^{+/+}$ (n=5)	Liver Sulf1$^{-/-}$ (n=7)	SA	Small Intestine Sulf1$^{+/+}$ (n=7)	Small Intestine Sulf1$^{-/-}$ (n=7)	SA	Lung Sulf1$^{+/+}$ (n=6)	Lung Sulf1$^{-/-}$ (n=7)	SA
ΔDi-0S + ΔDi-HA	26.0 ± 0.5	24.9 ± 0.4	#	13.9 ± 2.4	11.2 ± 0.3	#	33.5 ± 0.9	35.7 ± 0.6		35.9 ± 1.1	36.2 ± 0.8	
ΔDi-4S	68.9 ± 0.5	70.1 ± 0.4	#	56.6 ± 1.1	57.5 ± 0.5	#	57.6 ± 0.8	55.4 ± 0.7	*	49.0 ± 0.9	46.6 ± 0.5	*
ΔDi-6S	2.8 ± 0.1	2.6 ± 0.0	* #	1.0 ± 0.1	0.8 ± 0.0	**	1.4 ± 0.1	1.3 ± 0.0		8.5 ± 0.4	9.3 ± 0.2	
ΔDi-diS$_E$	1.1 ± 0.1	1.2 ± 0.0	*	26.8 ± 1.6	28.9 ± 0.5	#	6.3 ± 0.5	6.7 ± 0.3		4.3 ± 0.5	5.8 ± 0.2	*
ΔDi-diS$_D$	1.2 ± 0.0	1.2 ± 0.0	#	1.1 ± 0.1	1.2 ± 0.1		1.0 ± 0.1	0.9 ± 0.0		2.3 ± 0.1	2.2 ± 0.1	
ΔDi-triS	0.8 ± 0.3	0.9 ± 0.2		1.1 ± 0.1	0.9 ± 0.2		0.9 ± 0.2	0.7 ± 0.2		1.5 ± 0.5	1.6 ± 0.4	

Disaccharides	Kidney Sulf1$^{+/+}$ (n=7)	Kidney Sulf1$^{-/-}$ (n=7)	SA	Spleen Sulf1$^{+/+}$ (n=7)	Spleen Sulf1$^{-/-}$ (n=7)	SA	Testis Sulf1$^{+/+}$ (n=7)	Testis Sulf1$^{-/-}$ (n=7)	SA	Muscle Sulf1$^{+/+}$ (n=6)	Muscle Sulf1$^{-/-}$ (n=7)	SA
ΔDi-0S + ΔDi-HA	13.5 ± 0.6	13.5 ± 0.2	#	9.1 ± 0.3	8.5 ± 0.7	#	5.3 ± 0.4	4.8 ± 0.4		80.0 ± 0.6	82.0 ± 0.5	*
ΔDi-4S	60.4 ± 0.4	61.2 ± 0.4		79.4 ± 0.6	80.4 ± 1.3		72.1 ± 0.9	70.4 ± 0.7		18.1 ± 0.5	16.3 ± 0.5	*
ΔDi-6S	13.3 ± 0.3	12.3 ± 0.4	*	4.3 ± 0.2	3.2 ± 0.4	*	10.7 ± 0.5	11.6 ± 0.2		0.6 ± 0.0	0.6 ± 0.0	
ΔDi-diS$_E$	10.8 ± 0.4	11.1 ± 0.2		6.6 ± 0.4	7.4 ± 0.4		8.4 ± 1.0	9.7 ± 1.0		0.0	0.0	
ΔDi-diS$_D$	1.8 ± 0.1	1.8 ± 0.0		0.5 ± 0.1	0.4 ± 0.0		3.4 ± 0.2	3.4 ± 0.1		1.3 ± 0.1	1.1 ± 0.0	#
ΔDi-triS	1.3 ± 0.3	1.3 ± 0.3		0.4 ± 0.1	0.3 ± 0.1		2.5 ± 0.5	2.4 ± 0.6		0.8 ± 0.2	0.8 ± 0.2	

Data are means ± S.E.M. of each disaccharide unit in total CS+HA (%) for each organ. Statistical analysis (SA) done by the Student's *t*-test reveals significant difference between *Sulf1*-deficient mice and the wild-type controls (* $P < 0.05$, ** $P < 0.01$). # indicates that Welch's *t*-test was used because 2 groups had unequal variances.

Table S2. CS disaccharide composition in *Sulf2* knockout mouse organs

Disaccharides	Brain			Liver			Small Intestine			Lung		
	Sulf2 [+/+] (n = 7)	*Sulf2* [-/-] (n = 7)	SA	*Sulf2* [+/+] (n=7)	*Sulf2* [-/-] (n=6)	SA	*Sulf2* [+/+] (n=7)	*Sulf2* [-/-] (n=7)	SA	*Sulf2* [+/+] (n=7)	*Sulf2* [-/-] (n=6)	SA
ΔDi-0S + ΔDi-HA	20.4 ± 1.6	21.7 ± 2.1		13.1 ± 1.2	14.3 ± 1.2		39.2 ± 2.3	40.0 ± 1.2		36.4 ± 1.2	34.8 ± 1.8	
ΔDi-4S	76.1 ± 1.5	74.5 ± 2.2		59.8 ± 1.5	59.8 ± 2.3		50.7 ± 2.3	50.3 ± 1.8		47.6 ± 1.5	48.3 ± 1.4	
ΔDi-6S	1.5 ± 0.6	1.6 ± 0.5		0.5 ± 0.2	0.6 ± 0.2		1.2 ± 0.4	1.1 ± 0.4		7.3 ± 0.6	7.8 ± 0.8	
ΔDi-diS$_E$	1.1 ± 0.1	1.2 ± 0.2		26.1 ± 2.2	24.7 ± 3.0		8.5 ± 0.4	8.1 ± 0.6		7.9 ± 0.5	8.3 ± 0.7	
ΔDi-diS$_D$	0.9 ± 0.0	0.9 ± 0.1		0.3 ± 0.1	0.3 ± 0.2		0.4 ± 0.2	0.5 ± 0.2		0.9 ± 0.3	0.9 ± 0.2	
ΔDi-triS	0.6 ± 0.2	0.7 ± 0.2		0.2 ± 0.1	0.2 ± 0.1		0.4 ± 0.2	0.4 ± 0.2		0.8 ± 0.3	0.8 ± 0.3	

Disaccharides	Kidney			Spleen			Testis			Muscle		
	Sulf2 [+/+] (n=7)	*Sulf2* [-/-] (n=7)	SA	*Sulf2* [+/+] (n=7)	*Sulf2* [-/-] (n=7)	SA	*Sulf2* [+/+] (n=7)	*Sulf2* [-/-] (n=7)	SA	*Sulf2* [+/+] (n=6)	*Sulf2* [-/-] (n=6)	SA
ΔDi-0S + ΔDi-HA	21.9 ± 2.4	20.0 ± 2.1		9.6 ± 0.5	8.9 ± 0.6		5.3 ± 0.3	5.2 ± 0.3		77.9 ± 2.7	78.0 ± 2.5	
ΔDi-4S	54.1 ± 2.0	53.7 ± 2.0		78.3 ± 1.4	79.6 ± 1.4		67.7 ± 1.4	68.2 ± 1.8		18.9 ± 2.3	18.9 ± 2.2	
ΔDi-6S	12.4 ± 0.6	13.2 ± 0.7		2.8 ± 0.5	2.1 ± 0.6		10.4 ± 0.7	10.3 ± 0.9		0.4 ± 0.2	0.4 ± 0.1	
ΔDi-diS$_E$	10.3 ± 1.0	11.7 ± 1.0		9.1 ± 0.9	9.2 ± 0.5		14.9 ± 1.1	14.7 ± 1.2		1.9 ± 0.5	1.8 ± 0.4	
ΔDi-diS$_D$	1.3 ± 0.3	1.3 ± 0.2		0.2 ± 0.1	0.2 ± 0.1		1.4 ± 0.4	1.5 ± 0.4		0.9 ± 0.2	0.9 ± 0.2	
ΔDi-triS	1.1 ± 0.4	1.0 ± 0.3		0.2 ± 0.1	0.1 ± 0.1		1.5 ± 0.4	1.4 ± 0.5		0.7 ± 0.2	0.7 ± 0.2	

Data are means ± S.E.M. of each disaccharide unit in total CS+HA (%) for each organ. Statistical analysis (SA) done by the Student's *t*-test reveals no significant difference between *Sulf2*-deficient mice and the wild-type controls.